Development/Plasticity/Repair

The Role of Galanin in Cerebellar Granule Cell Migration in the Early Postnatal Mouse during Normal Development and after Injury

Yutaro Komuro,[1] Ludovic Galas,[2] Yury M. Morozov,[3] Jennifer K. Fahrion,[1] Emilie Raoult,[2] Alexis Lebon,[2] Amanda K. Tilot,[4] Shin Kikuchi,[1] Nobuhiko Ohno,[1,5,6] David Vaudry,[2,7] Pasko Rakic,[3,8] and Hitoshi Komuro[1,3]

[1]Department of Neurosciences, Lerner Research Institute, Cleveland Clinic, Cleveland, Ohio 44195, [2]Regional Platform for Cell Imaging of Normandy, INSERM, Université de Rouen Normandie, 76000 Rouen, France, [3]Department of Neuroscience, Yale University School of Medicine, New Haven, Connecticut 06510, [4]Department of Genomic Medicine, Lerner Research Institute, Cleveland Clinic, Cleveland, Ohio 44195, [5]Division of Neurobiology and Bioinformatics, National Institute for Physiological Sciences, Aichi 444-8787, Japan, [6]Department of Anatomy, Division of Histology and Cell Biology, School of Medicine, Jichi Medical University, Tochigi 329-0498, Japan, [7]Neuropeptides, Neuronal Death and Cell Plasticity Team, Laboratory of Neuronal and Neuroendocrine Communication and Differentiation, INSERM U1239, Université de Rouen Normandie, 76000 Rouen, France, and [8]Kavli Institute for Neuroscience, Yale School of Medicine, New Haven, Connecticut 06510

Galanin, one of the most inducible neuropeptides, is widely present in developing brains, and its expression is altered by pathologic events (e.g., epilepsy, ischemia, and axotomy). The roles of galanin in brain development under both normal and pathologic conditions have been hypothesized, but the question of how galanin is involved in fetal and early postnatal brain development remains largely unanswered. In this study, using granule cell migration in the cerebellum of early postnatal mice (both sexes) as a model system, we examined the role of galanin in neuronal cell migration during normal development and after brain injury. Here we show that, during normal development, endogenous galanin participates in accelerating granule cell migration via altering the Ca^{2+} and cAMP signaling pathways. Upon brain injury induced by the application of cold insults, galanin levels decrease at the lesion sites, but increase in the surroundings of lesion sites. Granule cells exhibit the following corresponding changes in migration: (1) slowing down migration at the lesion sites; and (2) accelerating migration in the surroundings of lesion sites. Experimental manipulations of galanin signaling reduce the lesion site-specific changes in granule cell migration, indicating that galanin plays a role in such deficits in neuronal cell migration. The present study suggests that manipulating galanin signaling may be a potential therapeutic target for acutely injured brains during development.

Key words: **cerebellum; galanin; granule cell; live cell imaging; mice; neuronal migration**

Significance Statement

Deficits in neuronal cell migration caused by brain injury result in abnormal development of cortical layers, but the underlying mechanisms remain to be determined. Here, we report that on brain injury, endogenous levels of galanin, a neuropeptide, are altered in a lesion site-specific manner, decreasing at the lesion sites but increasing in the surroundings of lesion sites. The changes in galanin levels positively correlate with the migration rate of immature neurons. Manipulations of galanin signaling ameliorate the effects of injury on neuronal migration and cortical layer development. These results shed a light on galanin as a potential therapeutic target for acutely injured brains during development.

Received Mar. 8, 2015; revised Aug. 16, 2021; accepted Aug. 19, 2021.

Author contributions: Y.K., L.G., D.V., P.R., and H.K. designed research; Y.K., L.G., Y.M.M., J.K.F., E.R., S.K., N.O., D.V., and H.K. performed research; Y.K., J.K.F., E.R., A.L., and H.K. analyzed data; Y.K., A.K.T., and H.K. wrote the paper.

This work was supported by the Cleveland Clinic.

S. Kikuchi's present address: Department of Anatomy 1, Sapporo Medical University School of Medicine, Sapporo, Hokkaido 060-8556, Japan.

Y. Komuro's present address: Department of Neurology, David Geffen School of Medicine at UCLA, Los Angeles, CA 90095.

The authors declare no competing financial interests.

Correspondence should be addressed to Hitoshi Komuro at komuroh@ccf.org.

https://doi.org/10.1523/JNEUROSCI.0900-15.2021

Introduction

Galanin is a 29–30 aa, C-terminally amidated peptide initially isolated from porcine intestine (Mitsukawa et al., 2008; Lang et al., 2015). The N-terminal 1–15 aa of galanin are highly conserved (Lang et al., 2007). The actions of galanin are mediated via G-protein-coupled receptors—galanin receptor 1–3 (GalR1–3; Webling et al., 2012). Galanin is thought to regulate numerous physiological functions in the adult mammalian nervous system (Kinney et al., 2002; Lang et al., 2015) and to play a role in neurologic disorders

(Lundström et al., 2005), such as Alzheimer's disease (Steiner et al., 2001) and epilepsy (Mazarati, 2004).

Galanin is one of the most inducible neuropeptides (Holm et al., 2012). Its biosynthesis is increased 2- to 10-fold on axotomy in the periphery and on seizure activity in the brain (Mitsukawa et al., 2008). Galanin expression and signaling is also activated during neuronal injury and repair (Wynick and Bacon, 2002; Mahoney et al., 2003), suggesting the possible trophic action of galanin. Experimentally induced focal ischemia in rat cerebra increases galanin and GalR1 mRNAs (Shen and Gundlach, 2010). The injection of galanin agonists inhibits seizures (Mazarati et al., 2004). A novel *de novo* mutation (p.A39E) in the GAL gene impairs galanin signaling in the hippocampus, leading to temporal lobe epilepsy (Guipponi et al., 2015).

The possible role of galanin in brain development has been hypothesized. Galanin is abundantly expressed in the developing brain (Elmquist et al., 1993; Ryan et al., 1997; Shen et al., 2003, 2005), and immature neurons express GalR1–3 (Burazin et al., 2000; Shen et al., 2005; Abbosh et al., 2011). *GAL* mRNA is detected in proliferative zones of neuronal and glial precursors and migratory routes of immature neurons in developing brains (Shen et al., 2003), suggesting that galanin may play a role in controlling the proliferation and migration of neurons.

In this study, we determined whether galanin plays a role in neuronal migration during normal development and under pathologic conditions. In the developing brain, immature neurons migrate from the birthplace to the final destinations, where they reside the rest of their lives (Rakic, 1990). This translocation of immature neurons is essential for the formation of cortical layers and nuclei (Rakic, 1990; Flint and Kriegstein, 1997; Marín and Rubenstein, 2003). The deficits in neuronal migration lead to a variety of neurologic disorders (Manent et al., 2009; Valiente and Marín, 2010).

To test the role of galanin in neuronal migration during brain development, we used the migration of cerebellar granule cells as a model system. Cerebellar granule cells, small excitatory interneurons, are the most abundant type of neurons and exhibit the stereotypic pattern of migration. In the early postnatal cerebellum [postnatal day 5 (P5) to P15 in mice], postmitotic granule cells migrate from the birthplace [external granular layer (EGL)] through the molecular layer (ML), and the Purkinje cell layer (PCL) to reach the final destination within the internal granular layer (IGL; Komuro and Yacubova, 2003; Komuro et al., 2013). Granule cell precursors and postmitotic granule cells express all three types of galanin receptors (Jungnickel et al., 2005), and the levels of GalR1 mRNA are significantly higher at P10 (a peak of granule cell migration) than at all other ages (Jungnickel et al., 2005).

To test the role of galanin in neuronal migration under pathologic conditions, we induced focal brain damage using freezing treatment (FT), which produces focal cortical disorganization (e.g., focal microgyria) in the developing brain without cellular abnormality (Peiffer et al., 2003; Scantlebury et al., 2004; Chiaretti et al., 2011; Wang et al., 2014). The focal cortical disorganization suggests the deficits in neuronal cell migration.

The use of time-lapse imaging of granule cell migration *in vitro* and *in vivo* revealed that galanin plays a role in accelerating granule cell migration via the activation of its receptors. Furthermore, FT resulted in lesion site-specific alterations of granule cell migration by inducing corresponding alterations of galanin levels.

Materials and Methods

Animals. We used embryonic and early postnatal CD-1 mice (both sexes). All animal procedures were approved by the Internal Animal Care and Use Committee of the Cleveland Clinic Foundation and The University of Rouen Normandy.

Observation of granule cell migration in microexplant cultures. Monitoring of granule cell migration in microexplant cultures of early postnatal mouse cerebella was performed as described previously (Yacubova and Komuro, 2002; Kumada et al., 2009; Raoult et al., 2011; Li et al., 2012). Cerebella of P3 mice were quickly removed from the skull, placed in cold HBSS (Sigma-Aldrich), and freed from meninges and choroid plexus. Cerebellar slices were then made with a surgical blade from which white matter (WM) and deep cerebellar nuclei were removed. Rectangular pieces (50–100 μm) were dissected out from the remaining tissue, which mainly consisted of the cerebellar gray matter. The microexplants were rinsed with the culture medium and placed on 35 mm glass-bottom microwell dishes (1 microexplant/dish; MatTek) with 50 μl of the culture medium. The culture medium consisted of Neurobasal Medium (Thermo Fisher Scientific) with N2 supplement (Thermo Fisher Scientific), 90 U/ml penicillin, and 90 μg/ml streptomycin. Each dish was placed in a CO_2 incubator (37°C, 95% and 5% CO_2). The glass-bottom microwell dishes were coated with poly-L-lysine (100 μg/ml)/laminin (20 μg/ml) before use. Two hours after plating, 1.5 ml of the culture medium was added to each dish. Twenty hours after plating, dishes were transferred into the chamber of a microincubator attached to the stage of a confocal microscope (model SP5, Leica). The chamber temperature was kept at 37.0 ± 0.5°C using a temperature controller (catalog #TC-202, Medical Systems Corp.) during the observation of migration. The cells were provided with constant gas flow (95% air, 5% CO_2). Granule cells were illuminated with a 488 nm wavelength light from an argon laser through an inverted microscope equipped with a 20× oil-immersion objective, and the light transmitted through granule cells was detected by a photomultiplier. Images of granule cells in a single focal plane were collected every 60 s. To test the role of galanin in granule cell migration, each chemical was added to the culture medium in a separate experiment. The distance of granule cell migration before and after the application of each chemical was analyzed using ImageJ software (NIH).

Measurement of intracellular Ca^{2+} levels of migrating granule cells. Monitoring of changes in intracellular Ca^{2+} levels of migrating granule cells in microexplant cultures was performed as described previously (Komuro and Rakic, 1996; Yacubova and Komuro, 2002; Kumada and Komuro, 2004). Small pieces of P3 mouse cerebellum were placed on 35 mm glass-bottom microwell dishes that had been coated with poly-L-lysine (100 μg/ml)/laminin (20 μg/ml). Each dish was put in a CO_2 incubator (37°C, 95% air, 5% CO_2). The incubation medium consisted of Neurobasal Medium (Thermo Fisher Scientific) with N2 supplement (Thermo Fisher Scientific), 90 U/ml penicillin, and 90 μg/ml streptomycin. One day after plating, granule cells were incubated for 30 min with the cell-permeant, acetoxymethyl ester form of 1 μM Oregon Green 488 BAPTA-1 (Thermo Fisher Scientific) diluted in the culture medium. The cells were subsequently washed three times with the culture medium, and the dye was allowed to de-esterify for an additional 30–60 min in the CO_2 incubator. A confocal microscope (model SP5, Leica) was used to examine changes in intracellular Ca^{2+} levels. The granule cells loaded with Oregon Green 488 BAPTA-1 were illuminated with a 488 nm wavelength light, and fluorescence images for Ca^{2+} measurements (at 530 ± 15 nm) were collected every 1–10 s for up to 2 h. The changes in the fluorescence intensity of each granule cell were normalized to its baseline fluorescent intensity.

Observation of granule cell migration in cerebellar slices. Monitoring of granule cell migration in acute cerebellar slices of early postnatal mouse cerebella was performed as described previously (Cameron et al., 2007; Fahrion et al., 2012; Raoult et al., 2014). Cerebella of P10 mice were sectioned transversely or sagittally into 150-μm-thick slices on a vibrating blade microtome (model VT1000S, Leica Instruments). To label granule cells, cerebellar slices were incubated for 4 min in 2 μM Cell Tracker Green CMFDA (5-chloromethylfluorescein diacetate; Thermo

Fisher Scientific), which was added to the culture medium. The culture medium consisted of Neurobasal Medium (Thermo Fisher Scientific) with N2 supplement (Thermo Fisher Scientific), 90 U/ml penicillin, and 90 μg/ml streptomycin. The slices were subsequently washed with the culture medium and put into a CO_2 incubator. Two hours after labeling, slices were transferred into the chamber of a microincubator attached to the stage of a confocal microscope (model SP5, Leica). The distance of granule cell movement is closely related to the temperature of the medium; lowering the medium temperature slows cell movement (Rakic and Komuro, 1995). Therefore, the chamber temperature was kept at 37.0 ± 0.5°C using a temperature controller (catalog #TC-202, Medical Systems Corp.), and the slices were provided with constant gas flow (95% O_2, 5% CO_2). A confocal microscope (model SP5, Leica) was used to visualize migrating granule cells labeled with Cell Tracker Green CMFDA in the slices. The tissue was illuminated with a 488 nm wavelength light from an argon laser through an epifluorescence inverted microscope equipped with a 40× oil-immersion objective (numerical aperture, 1.25; Leica), and fluorescence emission was detected at 530 ± 15 nm. To clearly resolve the movement of granule cells, image data were typically collected at an additional electronic zoom factor of 1.5–2.0. Images of Cell Tracker Green CMFDA-labeled granule cells in a single focal plane or up to 20 different focal planes along the *z*-axis were collected with laser scans every 5–30 min for up to 4 h. At the beginning and end of each recording session for each preparation, frame images were recorded with 40× magnification (electronic zoom factor, 1), or 20× magnification (electronic zoom factor, 1) to determine the orientation of the slice preparations, the borders of cortical layers (the EGL, the ML, and the IGL), and the position of granule cells by optical sectioning of several different focal planes along the *z*-axis.

Real-time observation of granule cell migration in vivo. Monitoring of granule cell migration in early postnatal mice was performed as described previously (Fahrion et al., 2012; Li et al., 2012). Mice were deeply anesthetized by intraperitoneal injection of urethane (1 mg/g body weight). The skin and bone coverings on the dorsal surface of cerebella were surgically removed under a dissecting microscope. A small volume of 1,1′-dioctadecyl-3,3,3′,3′-tetramethylindocarbocyanine perchlorate (DiI) solution (Thermo Fisher Scientific) was injected into the EGL of lobules V, VIa, VIb, VII, and crus I of the cerebellum through glass electrodes with the use of a pressure injection system. Then, warmed gelatin was applied to the surface of the cerebellum and the incision site was sealed with a cover glass by dental glue. One hour after DiI injection, the mice were transferred to the stage of a confocal microscope (model SP5, Leica) and were held dorsal-side down on the stage. Using a heating pad, the rectal temperature of animals was maintained at 37.0°C during the entire period of observation. A confocal microscope was used to visualize the tangential migration of DiI-labeled granule cells in the EGL. Images of DiI-labeled granule cells were collected every 3–10 min for up to 4 h. Anesthesia wearing off caused problems for monitoring granule cell migration over time. To avoid this potential problem, throughout the observation session, animals were monitored every 30 min for changes in respiratory rate, return of toe withdrawal reflexes, or any other body movement. Any of the indications that the anesthesia was wearing off were followed by supplemental injections of urethane (0.3 mg/g body weight). The distance of granule cell migration was analyzed using ImageJ software.

Freezing treatment on the cerebellum of P10 mice. Pups (P10) were anesthetized with isoflurane (2%) in room air, and a small incision was made in the anteroposterior plane of the skin over the cerebellum. A cooled (−70°C) 1-mm-diameter platinum probe was placed on the midline of occipital bone near the border between occipital bone and interparietal bone for 10 s. Animals receiving sham surgery were treated identically to those receiving freezing treatment except that the probe was maintained at room temperature. After placement of the probe, the incision was sutured. The mice recovered from anesthesia in a warm box.

Immonohistochemical analysis of embryonic and early postnatal mouse brains. After an anesthetic overdose, early postnatal mice (P6, P10, P11, and P12) were perfused transcardially with PBS, pH 7.4, followed by 4% paraformaldehyde (PFA) in PBS. Brains were quickly dissected and postfixed overnight at 4°C with the same fixative solution. In the case of embryonic day 16 (E16) mouse embryos, brains were isolated from embryos and were fixed in 4% PFA in PBS at 4°C for 4 h. Brains of both embryonic mice and early postnatal mice were stored for 12 h in a solution of PBS containing 15% and 30% sucrose successively. Thereafter, the brains were cut at 12 μm in the sagittal plane, transverse plane, or coronal plane with a cryostat (model CM 3050 S, Leica). Tissue sections were mounted on glass slides coated with 0.5% gelatin and 5% chrome alum. Before immunofluorescence analysis, the tissue sections were rinsed in PBS, and background was blocked by incubation for 1 h in 3% normal donkey serum (Jackson ImmunoResearch) in PBS with 0.1% Triton X-100, followed by overnight incubation at 4°C in blocking solution with the primary antibody. The following primary antibodies were used: galanin (rabbit; dilution, 1:500; catalog #AB2233, EMD Millipore); calbindin D28 (goat; dilution, 1:300; catalog #sc-7691; Santa Cruz Biotechnology); GAD67 (mouse; dilution, 1:1000; catalog #ab26116, Abcam); α-synuclein (sheep; dilution, 1:500; catalog #ab6162, Abcam); Iba1 (goat; dilution, 1:500; catalog #NB100-1028, Novus Biologicals); and NG2 (rat; dilution, 1:500; catalog #546930, Thermo Fisher Scientific). The tissue sections were rinsed three times in PBS and incubated for 90 min at room temperature in blocking solution with Alexa Fluor 488-, 568-, and 594-conjugated donkey antibodies toward rabbit (1:1000; catalog #A32790, Thermo Fisher Scientific), goat (1:1000; catalog #A11057, Thermo Fisher Scientific), mouse (1:1000; catalog #A10037, Thermo Fisher Scientific), sheep (1:1000; catalog #A21099, Thermo Fisher Scientific), or rat IgG (1:1000; catalog #A21209, Thermo Fisher Scientific). The tissue sections were counterstained with DAPI (dilution, 1:1000; catalog #ab 228549, Abcam) for 10 min, followed by three washes with PBS. To study the specificity of the immunoreaction, the following controls were performed: (1) the use of isotype-specific Ig as a substitute for the primary antibodies; (2) substitution of antibodies with PBS; and (3) preincubation of the antibodies with synthetic peptides (Hewitt et al., 2014). Fluorescent images were observed with a confocal laser-scanning microscope (model TCS SP5, Leica).

Immunocytochemistry and correlative light/electron microscopy. P10 mice were perfused with a fixative containing 4% paraformaldehyde and 0.1% glutaraldehyde. Sagittal 60-μm-thick cerebellum sections were cut with a vibratome, cryoprotected in 30% sucrose, frozen with liquid nitrogen, washed in 0.05 M, pH 7.4, Tris buffer, and blocked with 5% bovine serum albumin. The sections were immersed in anti-galanin antibody (rabbit; dilution, 1:500; catalog #AB2233; EMD Millipore) overnight at room temperature. Biotinylated anti-rabbit IgGs (1:300) and the Elite ABC Kit (all from Vector Laboratories) with Ni-intensified 3,3′-diaminobenzidine-4HCl (DAB-Ni) as a chromogen were applied. Thereafter, sections were postfixed with 1% OsO_4, dehydrated in alcohol and propylene oxide, and then embedded in Durcupan ACM [Fluka (Buchs)] on microscope slides and coverslipped. Selected fragments of tissue were photographed using an Axioplan 2 Microscope (Zeiss) and then re-embedded into Durcupan blocks for electron microscopy (EM) investigation. The samples were cut with a Reichert ultramicrotome into 70-nm-thick sections, stained with uranyl acetate and lead citrate, and evaluated and photographed in a JEM 1010 electron microscope (JEOL) equipped with a Multiscan 792 digital camera (Gatan).

Measurement of cerebellar cortical layer growth. After an anesthetic overdose, mice of the control and FT groups were perfused transcardially with PBS, pH 7.4, followed by 4% paraformaldehyde in PBS. Brains were quickly dissected and postfixed overnight at 4°C with the same fixative solution. Brains were stored for 12 h in a solution of PBS containing 15% and 30% sucrose successively. Thereafter, brains were sectioned sagittally and transversely at 16 μm in a cryostat and placed on slides. Every sixth section was stained with cresyl violet. After staining, the sections were examined with a bright-field light microscope and photographed with a 10×, 20×, 63×, or 100× objective lens using a digital camera. Images of each cerebellar cortical layer in the sagittal and transverse sections were obtained. The width of each cerebellar cortical layer was analyzed using ImageJ software.

Measurement of cerebellar galanin levels. Measuring of cerebellar galanin levels was performed as previously described (Sakamoto et al., 2000). Lobule VIb and crus I of cerebella of control and FT mice were

dissected out 12, 24, and 48 h after treatment. The tissues were boiled for 7 min and homogenized in 5% acetic acid. The homogenate was centrifuged at 16,000 × *g* for 30 min at 4°C. The supernatant was collected into a tube, and the resulting precipitate was again homogenized and centrifuged. The two supernatants were then pooled and forced through a disposable C18 cartridge (Sep-Pak Vac 1 ml, Waters). The retained material was then eluted with 60% methanol. The eluate was concentrated in a vacuum centrifuge and subjected to ELISA. The galanin ELISAs (GAL ELISA Kit, TSZ ELISA) were used to measure galanin levels in the cerebellar samples according to manufacturer instructions. The galanin levels in lobule VIb and curs I on the cerebellum were normalized per the total number of milligrams of protein assayed.

Measurement of granule cell translocation using bromodeoxyuridine. Examination of granule cell translocation using bromodeoxyuridine (BrdU) was performed as described previously (Kumada et al., 2006; Fahrion et al., 2012). P10 mice were injected with BrdU (50 μg/g body weight, i.p.) 4 h before FT or sham treatment. All animals were transcardially perfused with 4% paraformaldehyde in PBS 48 h after treatment. Brains were postfixed in 4% paraformaldehyde in PBS for 24 h, stored in a 30% sucrose solution, and sectioned sagittally into 30-μm-thick slices. In each section, cells that had incorporated BrdU into their DNA were detected by an anti-BrdU monoclonal antibody (BrdU labeling and Detection Kit I, Boehringer Mannheim) and fluorescein-conjugated secondary antibody. Fluorescent signals were detected and processed using a confocal microscope.

Detection of apoptotic cell death using terminal deoxynucleotidyl transferase-mediated biotinylated UTP nick end labeling assay. Examination of apoptotic cell death of granule cell precursors and granule cells was performed as described previously (Kumada et al., 2006; Fahrion et al., 2012). All mice were transcardially perfused with 4% paraformaldehyde in PBS 48 h after FT or sham treatment. Brains were postfixed in 4% paraformaldehyde in PBS for 24 h, stored in a 30% sucrose solution, and sectioned sagittally or transversely into 16-μm-thick slices. In each section, the apoptotic cell death of granule cells and granule cell precursors was determined by the terminal transferase dUTP nick end labeling (TUNEL) Assay Kit (Millipore) according to the manufacturer instructions. Fluorescent signals were detected and processed using a confocal microscope.

Measurement of the number of $BrdU^+$ cells and $TUNEL^+$ cells in cerebellar cortical layers. Images of fluorescently labeled $BrdU^+$ cells and $TUNEL^+$ cells in up to 25 different focal planes (1 μm interval) along the *z*-axis were captured by a blinded observer with the use of a confocal microscope (model SP5, Leica). The laser intensity, the gain factor, and the offset factor of the confocal microscope were fixed and maintained throughout the image-taking process of all sections. At the beginning of each cell number-counting session for each section, transmitted images and fluorescent images were simultaneously recorded with 10× or 20× magnification to determine the orientation of the slice preparations, the cortical layer borders (the EGL–ML border, the ML–PCL border, the PCL–IGL border, and the IGL–WM border), and the position of $BrdU^+$ cells and $TUNEL^+$ cells within cerebellar cortical layers. After projecting the *z*-axis series images to single 2D frame images, the number of $BrdU^+$ cells and $TUNEL^+$ cells was manually counted in each section by using ImageJ software.

Golgi staining of migrating granule cells. Golgi staining of migrating granule cells was performed as described previously (Kumada et al., 2009). Cerebella of P10 mice were quickly removed from the skull and frozen with isopentane precooled to −70°C with dry ice. Then, cerebella were sectioned transversely into 90-μm-thick sections on a cryostat. Golgi staining was performed by using an FD Rapid GolgiStain Kit (FD NeuroTechnologies) according to the manufacturer instructions. After staining, the sections were examined with a bright-field light microscope and photographed with 40× or 63× oil-immersion objective lens using a digital camera.

Statistical analysis. Comparisons between groups were made using Two-tailed unpaired *t* test or one-way ANOVA followed by Tukey's *post hoc* test. A value of $p < 0.05$ was considered statistically significant. Data were expressed as the mean ± SD. The exact *N* (number of animals and cells) values are reported in parentheses on the bar graphs.

Results

Galanin accelerates granule cell migration *in vitro* via the activation of its receptors

To examine the role of galanin in granule cell migration, first, we determined whether the application of exogenous galanin alters the migratory behavior of granule cells. To this end, different concentrations of galanin ranging from 0.1 nM to 1 μM was added to the culture medium in microexplant cultures of P3 mouse cerebella. Real-time observation of cell movement demonstrated that the application of 100 nM galanin increases the migration distance of an isolated granule cell from 37.0 to 62.4 μm during the 30 min observational period (Fig. 1*A*,*B*). Although the application of 0.1 and 1 nM galanin did not significantly alter granule cell migration, the application of galanin ranging from 5 nM to 1 μM accelerated the migration by up to 55% of the control in a dose-dependent manner (Fig. 1*C*). The ED_{50} of galanin in the rate of granule cell migration was 8×10^{-9} M (Fig. 1*D*). Next, we examined whether galanin accelerates granule cell migration via the activation of its receptor. The application of 100 nM M40 (a nonselective galanin receptor antagonist) completely eliminated the effect of 1 μM galanin on the distance of granule cell migration (Fig. 2*A*). These results suggest that galanin accelerates granule cell migration in a dose-dependent manner through the activation of its receptors.

Galanin accelerates granule cell migration through alterations of Ca^{2+} signaling and cAMP signaling

Next, we examined the cellular mechanisms underlying galanin-induced acceleration of granule cell migration. Our working hypothesis was that galanin accelerates granule cell migration by altering Ca^{2+} and cAMP signaling. This is because it has been reported that the activation of galanin receptors stimulates the activity of phospholipase C (PLC), which increases Ca^{2+} release from intracellular Ca^{2+} stores through inositol triphosphate, and inhibits the activity of adenylate cyclase (AC), which is an upstream target of cAMP signaling (Lundström et al., 2005; Lang et al., 2007; Mitsukawa et al., 2008; Webling et al., 2012). Furthermore, it has been reported that the granule cell migration is highly sensitive to changes in the activity of Ca^{2+} and cAMP signaling pathways (Komuro and Rakic, 1993, 1996; Rakic et al., 1994; Kumada and Komuro, 2004; Kumada et al., 2006; Jiang et al., 2008; Komuro et al., 2015). First, the inhibition of PLC activity with U73122 (100 nM) or protein kinase C (PKC) activity, which is a downstream target of Ca^{2+} signaling, with calphostin C (10 nM), reduced the effects of 1 μM galanin on granule cell migration (Fig. 2*A*). Second, the stimulation of AC activity with forskolin (30 μM) or protein kinase A activity, which is a downstream target of cAMP signaling, with Sp-cAMPS (20 μM), decreased the effects of 1 μM galanin on granule cell migration (Fig. 2*A*). Together, these results suggest that galanin increases the distance of granule cell migration via stimulating Ca^{2+} signaling and inhibiting cAMP signaling.

Galanin increases spontaneous Ca^{2+} spikes in migrating granule cells

The involvement of Ca^{2+} signaling in galanin-induced acceleration of granule cell migration suggests that galanin may affect the occurrences of spontaneous Ca^{2+} spikes in granule cells, which are known to play a role in controlling granule cell migration (Komuro and Rakic, 1996; Kumada and Komuro, 2004; Komuro and Kumada, 2005). To test this possibility, using a Ca^{2+} indicator dye (Oregon Green 488 BAPTA-1), we examined whether

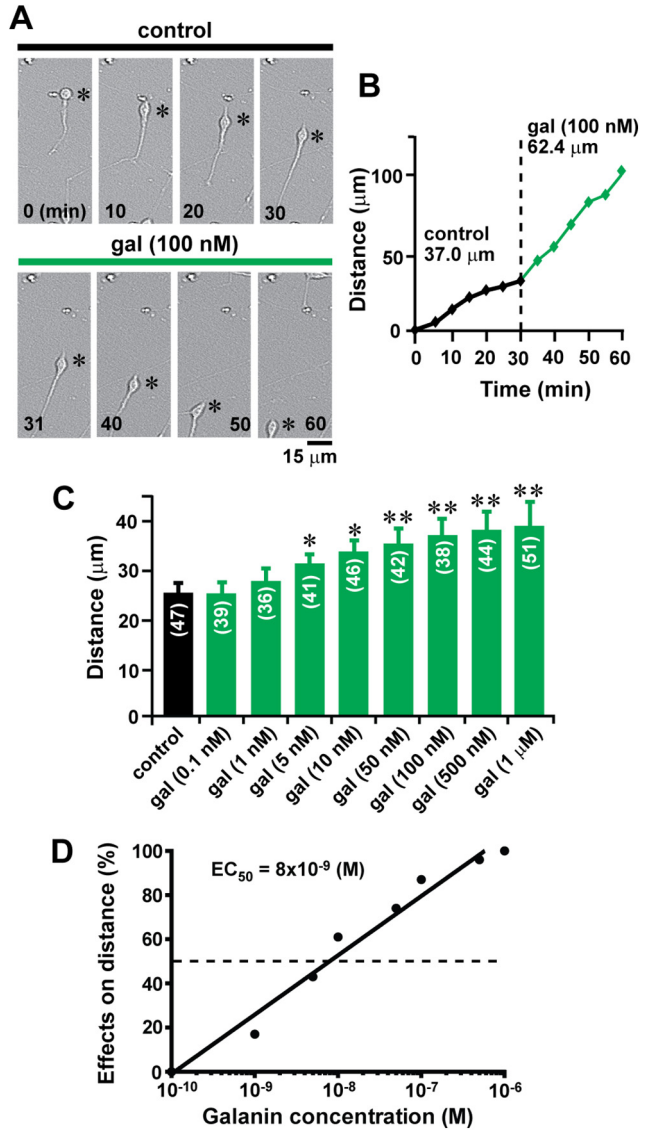

Figure 1. Galanin accelerates granule cell migration in a dose-dependent manner. ***A***, Time-lapse images showing that the application of 100 nM galanin increases the distance of granule cell migration in microexplant cultures of P3 mouse cerebella. Elapsed time (in minutes) is indicated on the bottom of each photograph. Asterisks mark granule cell somata. ***B***, The total distance traveled by the granule cell shown in ***A*** was plotted as a function of elapsed time before and after the application of 100 nM galanin. In this study, the average migration distance of granule cells during the 30 min observational period is ~25 μm (as presented in ***C***). To demonstrate the effects of galanin on migration distance of granule cells in ***A***, we selected the granule cells that migrated at the distance of 37 μm during the 30 min observational period before the application of galanin. Our previous study (Yacubova and Komuro, 2002) demonstrated that in the microexplant cultures, isolated granule cells exhibit a dynamic cycle of cell advancement and stationary phase every 3 h; active cell migration lasts for ~2 h, and a stationary period is ~1 h (Yacubova and Komuro, 2002). Granule cells also exhibit sequential and cyclic changes of the migration speed: fast-moving cells gradually slow down movement, while slow-moving cells gradually accelerate movement (Yacubova and Komuro, 2002). To demonstrate the effects of galanin on cell migration, we selected fast-moving granule cells, because our previous study (Yacubova and Komuro, 2002) suggested that, without any alterations of the microenvironment, fast-moving granule cells tend to slow down the speed of movement. As presented in ***A*** and ***B***, fast-moving granule cells increased the distance of migration from 37 μm during the 30 min observational period (before the application of galanin) to 62.4 μm during the 30 min observational period (after the application of galanin). These results suggest that observed changes in the distance of granule cell migration after the application of galanin is not because of the spontaneous fluctuations of the migration distance. ***C***, Histogram showing the effects of 0.1 nM to 1 μM galanin on the distance of granule cell migration in microexplant cultures of P3 mouse cerebella. The number in parentheses in each column indicates the number of granule cells tested.

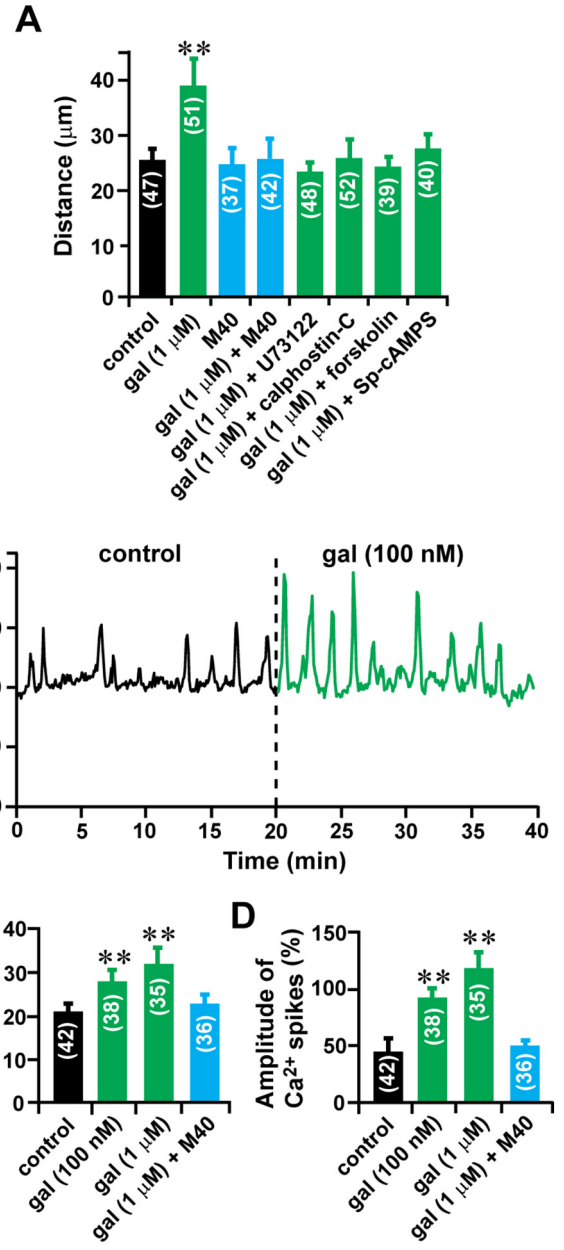

Figure 2. Galanin increases the frequency and amplitude of spontaneous Ca^{2+} spikes in migrating granule cells. ***A***, Histogram showing the effects of 1 μM galanin, 1 μM galanin + 30 μM forskolin, 1 μM galanin + 20 μM Sp-cAMPS, 1 μM galanin + 100 nM U73122, 1 μM galanin + 10 nM calphostin-C, 100 nM M40, and 1 μM galanin + 100 nM M40 on the distance of granule cell migration in microexplant cultures of P3 mouse cerebella. ***B***, Increase in spontaneous Ca^{2+} spikes in granule cell soma in microexplant cultures of P3 mouse cerebella by 100 nM galanin. ***C***, ***D***, Histograms showing changes in the frequency (***C***) and amplitude (***D***) of Ca^{2+} spikes in granule cell somata by 100 nM and 1 μM galanin or 1 μM galanin + 100 nM M40. The number in parentheses in each column indicates the number of granule cells tested. Error bars indicate SD. $^{**}p < 0.01$. In this series of experiments, 17 P3 CD-1 mice (both sexes) from two dams were used to prepare the microexplant cultures of cerebella.

←

Error bars indicate SD. $^{*}p < 0.05$; $^{**}p < 0.01$. ***D***, Histogram showing dose-dependent effects of galanin on the distance of granule cell migration. In this series of experiments, 18 P3 CD-1 mice (both sexes) from two dams were used to prepare the microexplant cultures of cerebella.

the application of exogenous galanin alters spontaneous Ca^{2+} spikes in migrating granule cells. The observation of changes in intracellular Ca^{2+} levels revealed that the application of 100 nM galanin increases the frequency and amplitude of spontaneous Ca^{2+} spikes in migrating granule cells in microexplant cultures of P3 mouse cerebella (Fig. 2*B*). On average, the application of galanin increased the frequency of Ca^{2+} spikes in migrating granule cells by 32% (100 nM) and 52% (1 μM) of the control, and the amplitude of Ca^{2+} spikes by 92% (100 nM) and 143% (1 μM) of the control (Fig. 2*C*,*D*). Galanin-induced changes in Ca^{2+} spikes in granule cells were eliminated by the application of 100 nM M40 (Fig. 2*C*,*D*). Because it has been reported that changes in the frequency and amplitude of Ca^{2+} spikes in granule cells are positively related to changes in the rate of granule cell migration (Komuro and Rakic, 1996), these results suggest that galanin accelerates granule cell migration by increasing the frequency and amplitude of spontaneous Ca^{2+} spikes.

The effects of galanin on granule cell migration do not depend on the mode of migration

In the early postnatal cerebellum, granule cells exhibit cortical layer-specific modes of migration (Komuro and Rakic, 1995, 1998a; Komuro et al., 2001). As schematically shown in Figure 3*A*, granule cells exhibit tangential migration in the EGL, glia-associated radial migration in the ML, and glia-independent radial migration in the IGL. One can expect that galanin may control granule cell migration in a cortical layer-dependent and migration mode-dependent manner. To address this issue, using acute cerebellar slice preparations obtained from P10 mouse cerebella, we examined the effects of the application of galanin in granule cell migration in three different cortical layers (EGL, ML, and IGL). The use of time-lapse recording of cell migration revealed that the application of 100 nM galanin increases the distance of granule cell migration in the ML from 18.1 to 25.6 μm during the 1 h observational period (Fig. 3*B*–*D*). The application of 100 nM or 1 μM galanin resulted in an increase in the distance of granule cell migration in all three cortical layers of P10 mouse cerebella in a dose-dependent manner (Fig. 3*E*). On average, the application of galanin accelerated granule cell migration in the EGL by 28% (100 nM) and 44% (1 μM) of the control, in the ML by 37% (100 nM) and 52% (1 μM) of the control, and in the IGL by 27% (100 nM) and 41% (1 μM) of the control (Fig. 3*E*). There was no statistical significance in the effects of galanin on the distance of granule cell migration among the EGL, ML, and IGL, indicating that the stimulative effects of galanin on granule cell migration do not depend on cerebellar cortical layers and the mode of migration.

Next, we examined whether endogenous galanin plays a role in granule cell migration. To answer this question, we examined the effects of M40 (a nonselective galanin receptor antagonist) on granule cell migration in the EGL, ML, and IGL. The application of 100 nM M40 reduced the average distance of granule cell migration in the EGL by 22% of the control, in the ML by 24% of the control, and in the IGL by 25% of the control (Fig. 3*E*). These results suggested that endogenous galanin plays a role in maintaining the rate of granule cell migration during their entire journey.

Expression of galanin in the early postnatal mouse cerebellum

To learn more about the roles of galanin in granule cell migration, using immunohistochemical tools, we examined the expression of galanin in the early postnatal mouse cerebellum during a

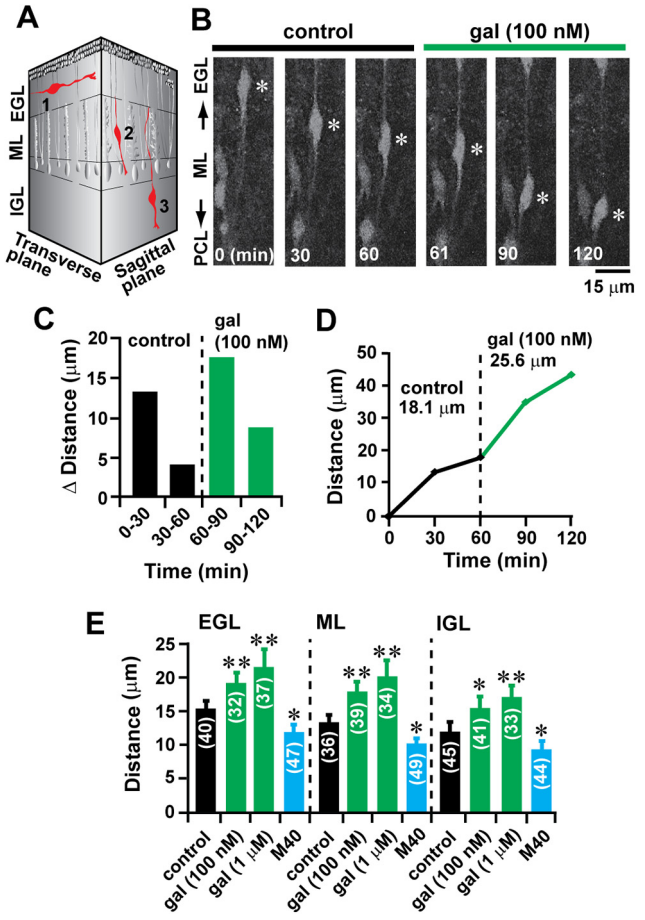

Figure 3. The effects of galanin on granule cell migration are independent of the mode of migration. ***A***, Schematic representation of the following three distinct modes of granule cell migration in the early postnatal mouse cerebellum: 1, tangential migration in the EGL; 2, glia-associated radial migration in the ML; and 3, glia-independent radial migration in the IGL. ***B***, Time-lapse images showing that the application of 100 nM galanin accelerates the radial migration of granule cells in the ML of P10 mouse cerebella. Elapsed time (in minutes) is indicated on the bottom of each photograph. Asterisks mark granule cell somata. The cortical layers and cortical layer borders (the EGL–ML border, the ML–PCL border, the PCL–IGL border, and the IGL–WM border) were determined by simultaneously taking transmitted images and Cell Tracker Green CMFDA fluorescent images at the beginning and end of each time-lapse recording session for cell migration by the use of a confocal microscope (model SP5, Leica). ***C***, ***D***, Sequential changes in the distance (***C***) traveled during each 30 min of the testing period and the total distance (***D***) by granule cell shown in ***B*** were plotted as a function of elapsed time before and after the application of 100 nM galanin. ***E***, Histogram showing the effects of 100 nM and 1 μM galanin, and 100 nM M40 on the distance of granule cell migration in the three cortical layers (the EGL, the ML, and the IGL) of P10 mouse cerebella. The number in parentheses in each column indicates the number of granule cells tested. Error bars indicate SD. $*p < 0.05$; $**p < 0.01$. In this series of experiments, 23 P10 CD-1 mice (both sexes) from three dams were used to prepare the 150-μm-thick slices of cerebella.

period of active granule cell migration. The low-magnification images revealed that during the peak of granule cell migration (at P10), galanin is present in every lobule (from lobule I to lobule X) of the cerebellum, and the expression of galanin is well colocalized with $GAD67^+$ regions (Fig. 4*A*). The high-magnification images suggested that several distinct types of neurons and neuronal processes express galanin in the developing cerebellar cortical layers (Fig. 4*B*–*H*). Galanin is expressed throughout the ML, and especially in the dendrites of $GAD67^+$ and $calbindin^+$ Purkinje cells (Fig. 4*B*,*C*). In the PCL, the somata of $GAD67^+$ and $calbindin^+$ Purkinje cells highly express galanin (Fig. 4*B*,*C*). In the IGL, galanin is expressed in the middle-sized somata of

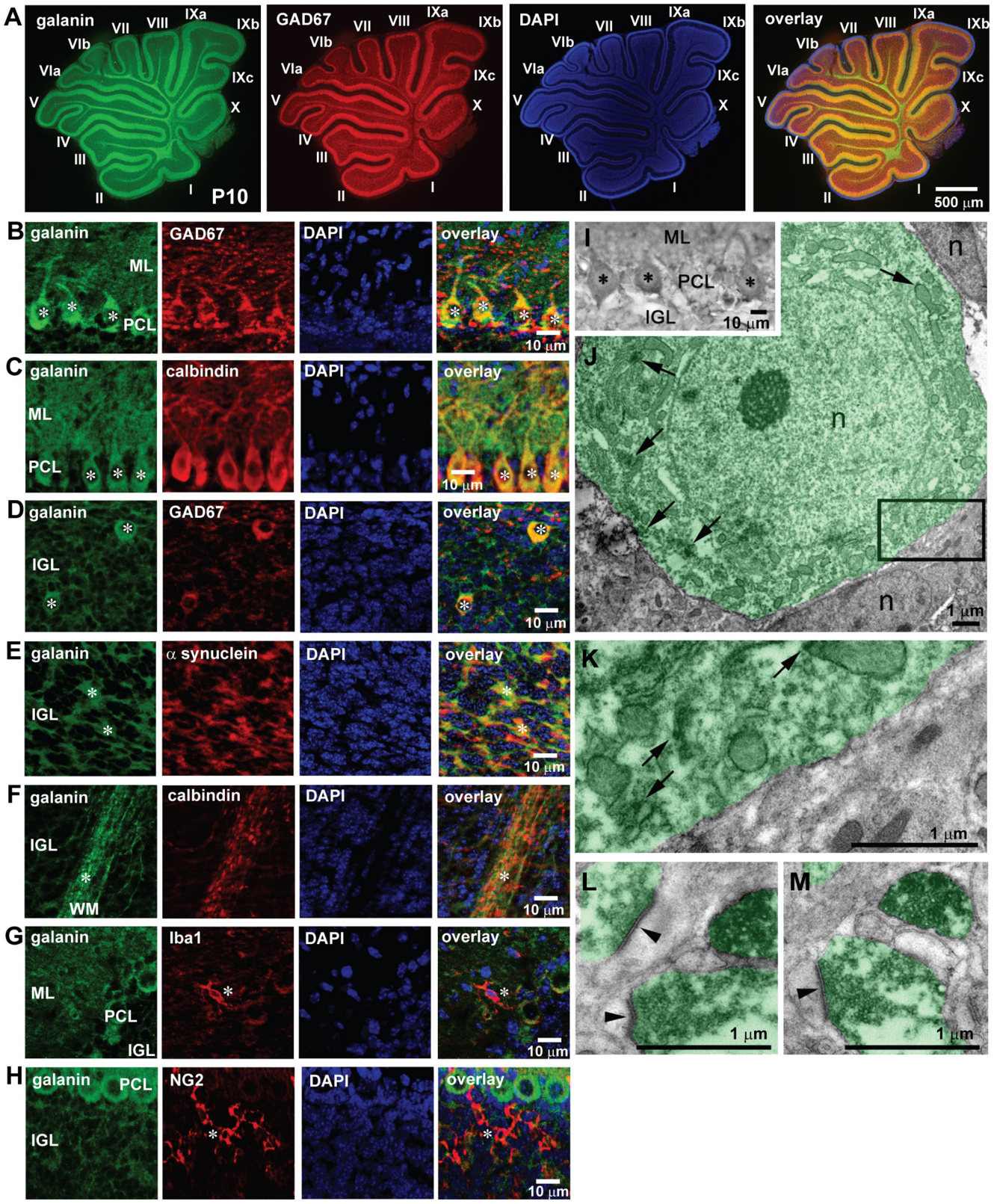

Figure 4. The expression of endogenous galanin in the P10 mouse cerebellum at the peak stage of granule cell migration. ***A***, Immunostains of galanin and GAD67 in the P10 mouse cerebellum. Galanin is expressed in all lobules (lobule I–X), and its expression is well colocalized with the expression of GAD67. ***B***, Immunostains showing the coexpression of galanin and GAD67 in the dendrites and somata of Purkinje cells (white asterisks) in the ML and the PCL. ***C***, Immunostains showing the coexpression of galanin and calbindin in the dendrites and somata of Purkinje cells (white asterisks) in the ML and the PCL. ***D***, Immunostains showing the coexpression of galanin and GAD67 in the cell somata marked by asterisks (possible Golgi cell somata) in the IGL. ***E***, Immunostains showing the coexpression of galanin and α-synuclein in the processes marked by asterisks (possible mossy fiber rosettes) in the IGL. ***F***, Immunostains showing the coexpression of galanin and calbindin in the axons marked by asterisks (possibly Purkinje cell axons) in the WM. ***G***, Immunostains showing the expression of galanin and Iba1 in the ML. Iba1$^+$ cells marked by an asterisk (microglia and macrophages) do not express galanin. ***H***, Immunostains showing the expression of galanin and NG2 in the IGL. NG2$^+$ cells marked by an asterisk (oligodendrocyte precursor cells) do not express galanin. In this series of experiments (from ***A*** to ***H***), ten P10 CD-1 mice (both sexes) from two dams were used to conduct immunohistochemical staining. ***I***,

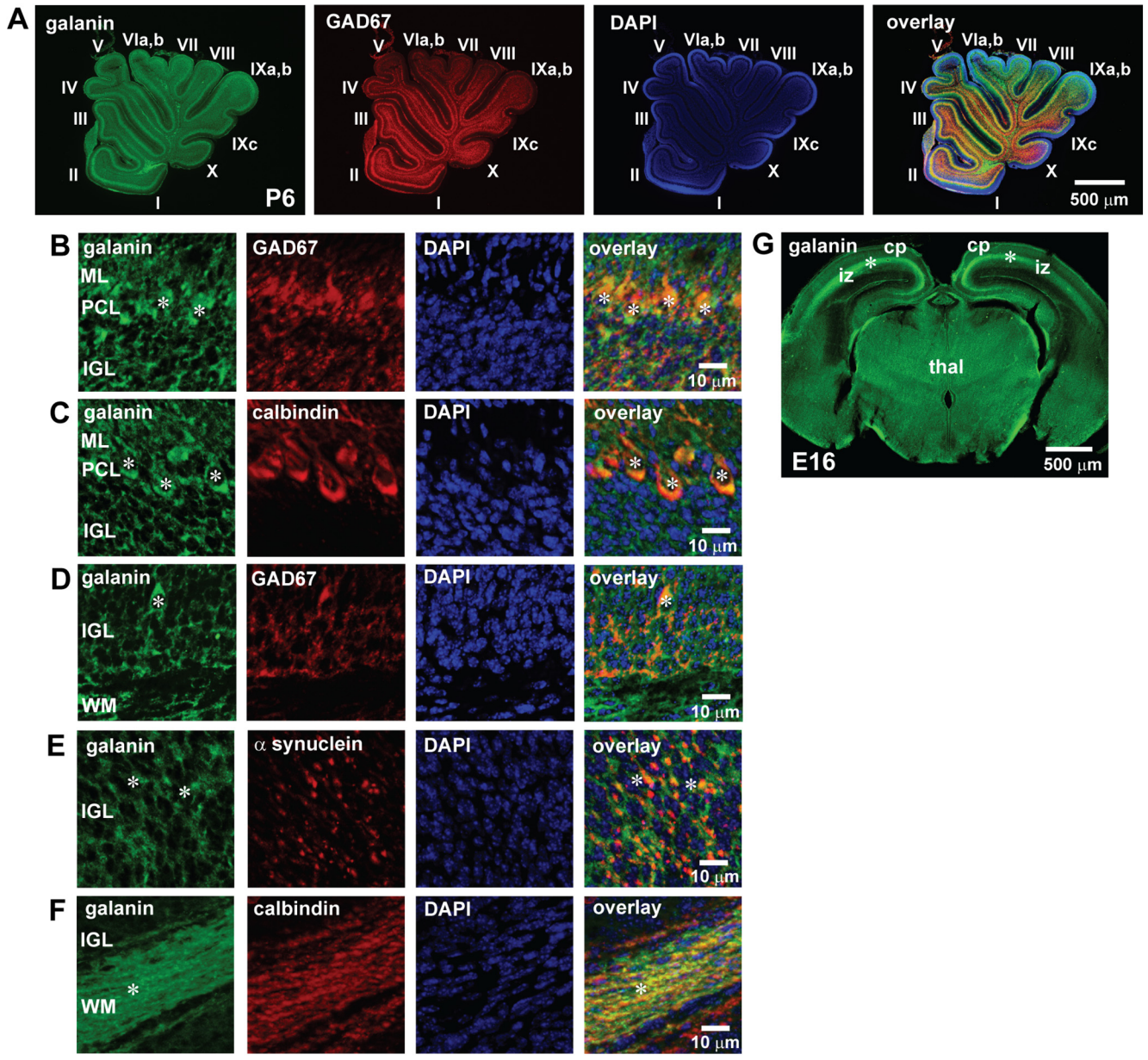

Figure 5. ***A–G***, The expression of endogenous galanin in the P6 mouse cerebellum (***A–F***) and the E16 mouse cerebrum (***G***). ***A***, Immunostains of galanin and GAD67 in the P6 mouse cerebellum. Galanin is expressed in all lobules (lobule I–X), and its expression is colocalized with the expression of GAD67. ***B***, Immunostains showing the coexpression of galanin and GAD67 in the dendrites and somata of Purkinje cells (white asterisks) in the ML and the PCL. ***C***, Immunostains showing the coexpression of galanin and calbindin in the dendrites and somata of Purkinje cells (white asterisks) in the ML and the PCL. ***D***, Immunostains showing the coexpression of galanin and GAD67 in the cell soma marked by asterisks (possible Golgi cell somata) in the IGL. ***E***, Immunostains showing the coexpression of galanin and α-synuclein in the processes marked by asterisks (possible mossy fiber rosettes) in the IGL. ***F***, Immunostains showing the coexpression of galanin and calbindin in the axons marked by asterisks (possibly Purkinje cell axons) in the WM. In this series of experiments (from ***A*** to ***F***), seven P6 CD-1 mice (both sexes) from two dams were used to conduct immunohistochemical staining. ***G***, Immunostains of galanin in the E16 mouse cerebrum. Galanin is expressed in the intermediate zone (marked by asterisks) in the cerebrum. cp, Cortical plate; thal, thalamus. In this series of experiments (***G***), three E16 CD-1 mice from two pregnant mice were used to conduct immunohistochemical staining.

←

Light microscopy images of galanin$^+$ Purkinje cells (asterisks), which were analyzed with electron microscopy. ***J***, Electron micrographs of a galanin$^+$ Purkinje cell body (highlighted semitransparent green). Accumulations of diffuse DAB-Ni staining in cytoplasm are indicated by arrows. N, Cell nucleus. ***K***, High-power image of the framed area (indicated in ***J***) shows contact of an immuno-negative cell with the galanin$^+$ Purkinje cell. Accumulations of diffuse DAB-Ni staining in cytoplasm are indicated by arrows. ***L***, ***M***, High-power images in the IGL show the expression of galanin in presynaptic terminals (highlighted semitransparent green). Arrowheads mark the synaptic sites. In this series of experiments (***I–M***), two P10 CD-1 mice (both sexes) from a single dam were used to conduct immuno-EM analysis.

GAD67$^+$ cells, which are likely Golgi cells (Fig. 4*D*), and α-synuclein$^+$ neuronal processes, which are likely mossy fiber terminals (mossy rosettes; Fig. 4*E*). In the WM, calbindin$^+$ neuronal processes, which are likely Purkinje cell axons, express galanin (Fig. 4*F*). In the developing cerebellar cortical layers, Iba1$^+$ cells (microglia/macrophages) and NG2$^+$ cells (oligodendrocyte progenitor cells) do not express galanin (Fig. 4*G*,*H*). Furthermore, analysis with the use of immuno-EM confirmed galanin expression in Purkinje cell somata and presynaptic terminals in the cerebellar cortical layers of P10 mice (Fig. 4*I–M*).

In the early postnatal cerebellum, the majority (~95%) of granule cells migrate from the EGL through the ML and the PCL

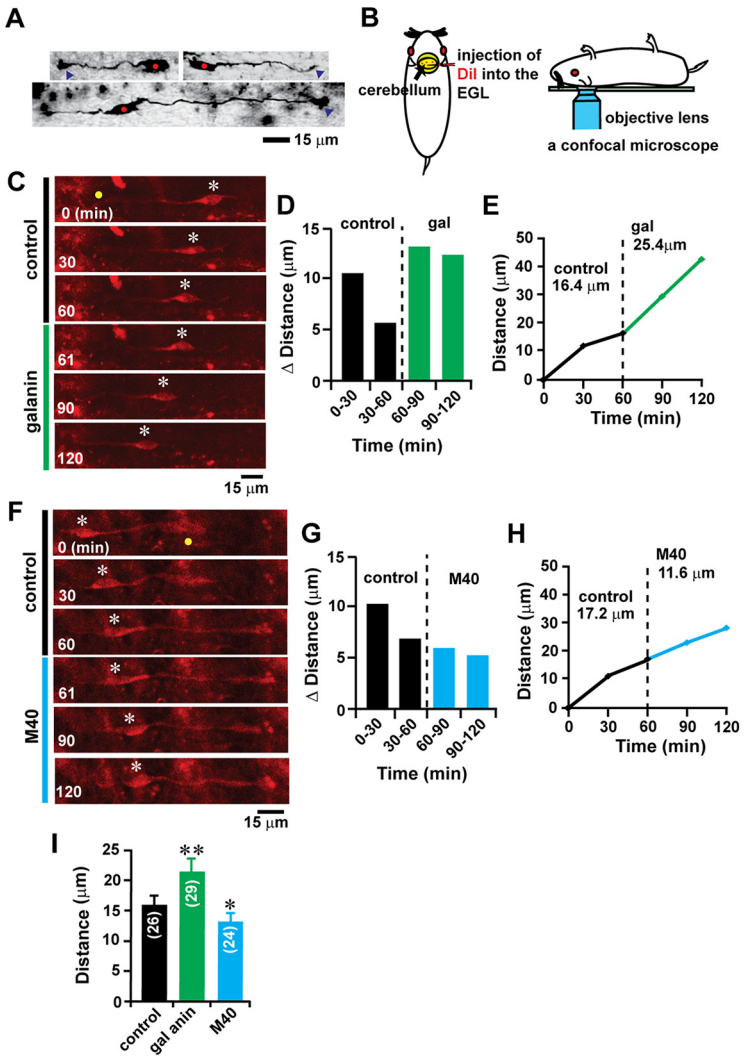

Figure 6. Alterations of granule cell migration *in vivo* by the application of galanin and M40. ***A***, Micrographs showing tangentially migrating granule cells in the EGL of P10 mouse cerebellum stained by the Golgi method. Red dots and blue arrowheads represent the somata and tips of leading processes of granule cells, respectively. ***B***, Schematic representation of the injection of fluorescent dye (DiI) into the EGL of the early postnatal mouse cerebellum and monitoring the migration of DiI-labeled granule cells *in vivo* using confocal microscopy. ***C***, Time-lapse images showing that the injection of galanin (10 μl of 1 μM) into the dorsal surface of P10 mouse cerebellum accelerates tangential migration of a DiI-labeled granule cell in the EGL. In ***C*** and ***F***, elapsed time (in minutes) is indicated on the bottom left corner of each photograph. Asterisks and yellow dots mark granule cell somata and the tip of leading processes, respectively. ***D***, ***E***, Sequential changes in the distance of granule cell migration during each 30 min interval (***D***) and the total distance of granule cell migration (***E***) shown in ***C*** were plotted as a function of elapsed time before and after the injection of galanin. ***F***, Time-lapse images showing that the injection of M40 (5 μl of 1 μM) into the dorsal surface of P10 mouse cerebellum decelerates tangential migration of a DiI-labeled granule cell in the EGL. ***G***, ***H***, Sequential changes in the distance of granule cell migration during each 30 min interval (***G***) and the total distance of granule cell migration (***H***) shown in ***F*** were plotted as a function of elapsed time before and after the injection of M40. ***I***, Histogram showing the effects of galanin and M40 on the distance of tangential migration of granule cells in the EGL of P10 mouse cerebella. The number in parentheses in each column indicates the number of granule cells tested. Error bars indicate SD. $*p < 0.05$; $**p < 0.01$. For the Golgi staining study, three P10 CD-1 mice (both sexes) from a single dam were used. For the study examining the effects of galanin on the *in vivo* migration of granule cells, 27 P10 CD-1 mice (both sexes) from nine dams were tested. Each experimental group (control group, galanin group, and M40 group) was composed of nine P10 CD-1 mice (both sexes) from the same nine dams.

to the IGL during the second postnatal week (Miale and Sidman, 1961). To examine whether galanin is expressed in the early stage of granule cell migration, we examined the expression of galanin in P6 mouse cerebellum. The low-magnification images revealed that in P6 mouse cerebella, galanin is already present in every lobule (from lobule I to lobule X) of the cerebellum in a similar pattern of distribution observed in P10 mouse cerebella (Fig. 5*A*). The low-magnification images indicated that in the cerebellar cortical layers of P6 mice, GAD67$^+$ and calbindin$^+$ Purkinje cells express galanin in the ML and the PCL (Fig. 5*B*,*C*). GAD$^+$ cells (possibly Golgi cells) and α-synuclein$^+$ neuronal processes (possibly mossy rosettes) express galanin in the IGL (Fig. 5*D*,*E*). Calbindin$^+$ processes (possibly Purkinje cell axons) express galanin in the WM (Fig. 5*F*). These results suggest that endogenous galanin is present in cerebellar cortical layers (the ML, the PCL, and the IGL) at the beginning of granule cell migration from the EGL to the IGL.

Furthermore, to determine whether the early expression of galanin during neuronal migration is limited to the cerebella, we examined the expression of galanin in the cerebrum of mouse embryos. Immunohistochemical staining revealed that at E16 (an active stage of migration of both cortical excitatory neurons and inhibitory neurons) of the mouse cerebra, galanin is present in the intermediate zone (iz; Fig. 5*G*), suggesting that endogenous galanin is present in the embryonic cerebrum, where many cortical neurons migrate through.

Role of galanin in granule cell migration *in vivo*

The expression of endogenous galanin in cerebellar cortical layers suggested that galanin might control cerebellar granule cell migration in the early postnatal mice. To test whether galanin plays a role in controlling granule cell migration *in vivo*, using an *in vivo* live-imaging system for cell migration (Fahrion et al., 2012; Li et al., 2012), we monitored the effect of the application of exogenous galanin and M40 on the tangential migration of granule cells in the EGL of P10 mouse cerebellum. At the middle and bottom of the EGL, postmitotic granule cells had a horizontally oriented soma with one or two horizontally extending processes (a leading process and a trailing process; Fig. 6*A*; Rakic, 1971; Kumada et al., 2009). To monitor granule cell migration in the EGL, a small amount of DiI solution was injected into the EGL of lobules V, VI, and VII of the P10 mouse cerebellum (Fig. 6*B*). Two hours after the DiI injection, the migration of DiI-labeled granule cells was observed using confocal microscopy (Fig. 6*B*). Time-lapse recordings of cell movement revealed that the injection of galanin (10 μl of 1 μM) into the dorsal surface of the cerebellum increases the distance of granule cell migration in the EGL of lobule VIb from 16.4 to 25.4 μm during the 1 h observational period (Fig. 6*C*–*E*). In contrast, the injection of M40 (5 μl of 1 μM) into the dorsal surface of the cerebellum decreased the distance of granule cell migration in the EGL of lobule VIb from 17.2 to 11.6 μm during the 1 h observational period (Fig. 6*F*–*H*). On average, in the EGL of lobules V, VI, and VII of the P10 mouse cerebellum, the injection of galanin (10 μl of 1 μM) increased the distance of granule cell migration by 34% of the control, while the injection of M40 (5 μl of 1 μM) decreased the

distance of migration by 18% of the control (Fig. 6*I*). These results suggest that in the early postnatal mouse cerebellum, the stimulation of galanin signaling accelerates granule cell migration, while the inhibition of galanin signaling decelerates the migration.

Focal freezing treatment on the skull alters the growth of cerebellar cortical layers in a lesion site-specific manner

After determining the role of galanin in granule cell migration *in vivo* and *in vitro*, we examined whether galanin also plays a role in granule cell migration after brain injury. To injure focal regions of the cerebellum, we applied FT on the skull of P10 mice (Chiaretti et al., 2011; Wang et al., 2014). As shown in Figure 7, *A* and *B*, a cooled (−70°) platinum probe (diameter, 1 mm) was placed on the midline of the occipital bone near the occipital bone–interparietal bone border of P10 mice for 10 s. In control animals (sham animals), the probe, which was maintained at room temperature, was placed on the same site of the occipital bone. Although FT did not affect the daily gain of body and cerebellar weight of mice (Fig. 7*C*,*D*), a histologic analysis revealed that 2 d after treatment, in the midline region of lobule VIb of FT mouse cerebella, the EGL, ML, and IGL are thinner compared with the control animals and the EGL is disorganized (Fig. 7*E–H*). In contrast, in the proximal regions of crus I of FT mouse cerebella, the EGL, ML, and IGL were thicker compared with those in the control animals (Fig. 7*E–H*). These results suggest that FT results in the undergrowth of cerebellar cortical layers in the midline regions of lobule VIb (the core of the lesion site, which is the region under the skull where the cooled probe is placed), but results in the overgrowth of cerebellar cortical layers in the proximal regions of lobule crus I (the surroundings of the lesion site).

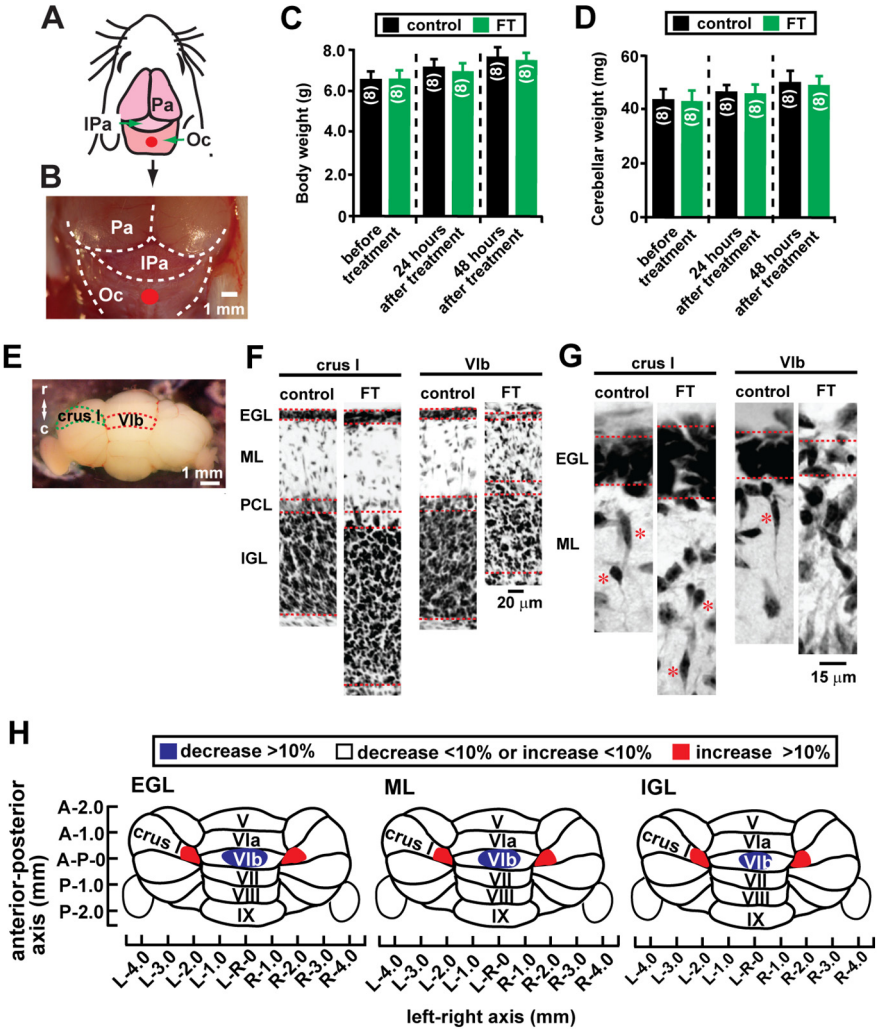

Figure 7. FT affects the growth of cerebellar cortical layers in a lesion site-specific manner. ***A***, Schematic representation showing the site (marked by a red circle) where a cooled (−70°C) 1-mm-diameter platinum probe was placed on the skull of a P10 mouse. IPa, Interparietal bone; Oc, occipital bone; Pa, parietal bone. ***B***, Micrograph showing the site (a red circle) of FT on the occipital bone (Oc) on P10 mouse. ***C***, ***D***, Histograms showing that FT does not affect daily gain of body weight (***C***) and wet cerebellar weight (***D***) 24 and 48 h after treatment compared with the control group. In ***C***, the number in parentheses in each column indicates the number of animals tested. In ***D***, the number in parentheses in each column indicates the number of cerebella tested. Error bars represent SD. ***E***, A dorsal view of P12 mouse cerebellum. Lobule VIb and left crus I are outlined by a dotted red line and a dotted green line, respectively. c, Caudal direction; r, rostral direction. ***F***, Low-magnification images of cresyl violet stains of the transverse sections of the cerebella of control and FT mice 48 h after treatment showing the alterations of the thickness of the EGL, the ML, the PCL, and the IGL of lobule VIb and left crus I. ***G***, High-magnification images of cresyl violet stains of the transverse sections of the cerebella of control and FT mice 48 h after treatment showing the disruption of the EGL of lobule VIb and the enlargement of the EGL of left crus I of the cerebella of FT mice. ***H***, Lesion site-specific changes in the growth of three cortical layer (the EGL, the ML, and the IGL) in the cerebella of FT mice 48 h after treatment. Positive changes (represented by red) and negative changes (represented by blue) in the growth of each cortical layer of FT mouse cerebella were calculated by dividing the width of each cortical layer in the FT mice by the width of each corresponding layer in the control mice. In the study examining the effects of FT on body weight (***C***), cerebellar weight (***D***), and the growth of cerebellar cortical layers (***E–H***), each experimental group (control group and FT group) was composed of 24 P10 CD-1 mice (both sexes) from the same six dams. Eight mice in each group were killed (1) before treatment, (2) 24 h after treatment, and (3) 48 h after treatment.

FT decelerates granule cell migration at the core of the lesion site, but accelerates granule cell migration at the surroundings of the lesion site

Next, using an *in vivo* live-imaging system for cell migration, we examined the effects of FT on granule cell migration. We focused on the migration of granule cells in the EGL of lobule VIb (the core of the lesion site) and crus I (the surroundings of the lesion site), and observed granule cell migration 12, 24, and 48 h after treatment. Compared with control mice, 12 h after treatment, FT mice exhibited a deceleration of granule cell migration in the midline region of lobule Vib and an acceleration of the migration in the proximal region of crus I (Fig. 8*A–H*). On average, the distance of granule cell migration in the midline region of lobule VIb in FT mice was reduced to 43% (12 h after treatment), 56% (24 h after treatment), and 66% (48 h after treatment) of the control group, while the distance of granule cell migration in the proximal region of left crus I in FT mice increased to 124% (12 h after treatment), 113% (24 h after treatment), and 105% (48 h after treatment) of the control group (Fig. 8*I*). These results suggest that FT decelerates granule cell migration at the core of the lesion

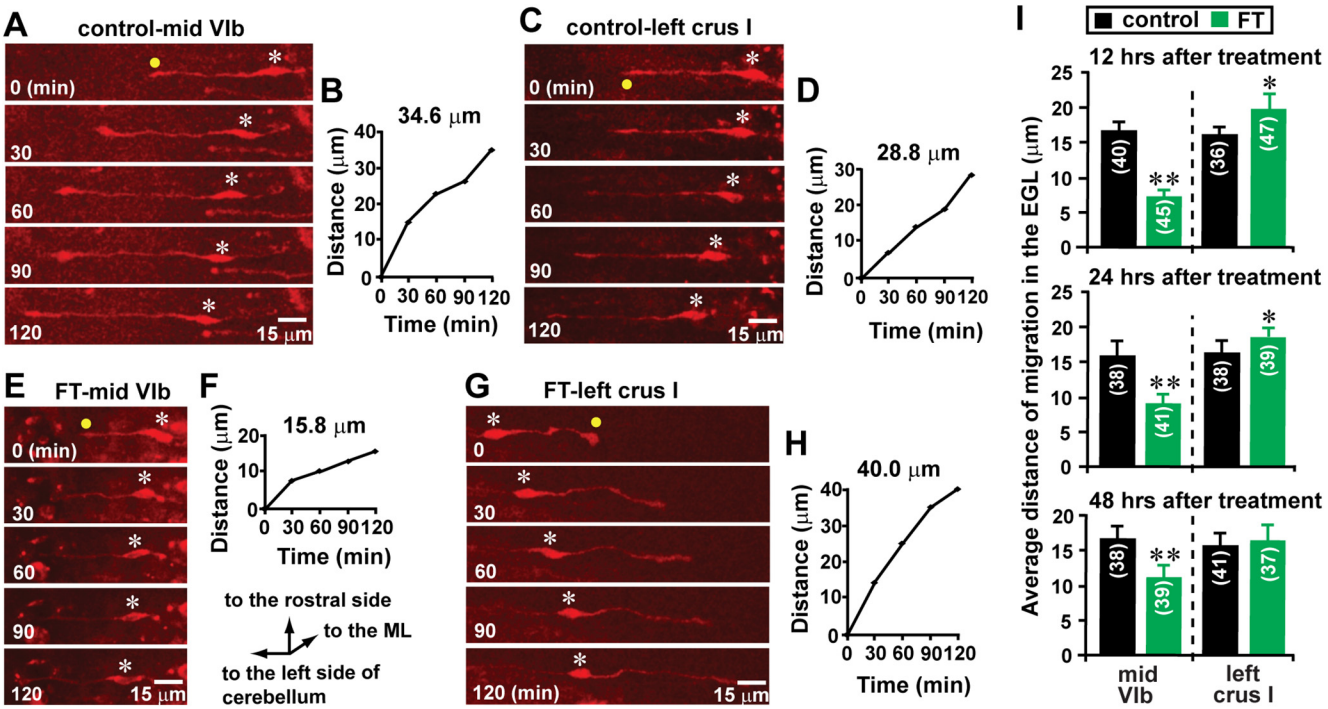

Figure 8. Lesion site-specific alterations of granule cell migration by FT. ***A***, ***C***, Time-lapse images showing tangential migration of granule cells in the EGL of the midline region of lobule VIb (***A***) and the proximal region of left crus I (***C***) of control mouse cerebella 12 h after sham treatment. Elapsed time (in minutes) is indicated on the bottom left corner of each photograph. Asterisks and yellow dots mark granule cell somata and the tip of leading processes, respectively. ***B***, ***D***, The total distance of granule cell migration during the 2 h observational period shown in ***A*** and ***C*** was plotted as a function of elapsed time. ***E***, ***G***, Time-lapse images showing tangential migration of granule cells in the EGL of the midline region of lobule VIb (***E***) and the proximal region of left crus I (***G***) of FT mouse cerebella 12 h after freezing treatment. Elapsed time (in minutes) is indicated on the bottom left corner of each photograph. Asterisks and yellow dots mark granule cell somata and the tip of leading processes, respectively. ***F***, ***H***, The total distance of granule cell migration during the 2 h observational period shown in ***E*** and ***G*** was plotted as a function of elapsed time. ***I***, Histogram showing the average distance of granule cell migration during the 1 h period in the EGL of the midline region of lobule VIb and the proximal region of left crus I in the control and FT mice 12, 24, and 48 h after treatment. The number in parentheses in each column indicates the number of granule cells tested. Error bars indicate SD. $^{*}p < 0.05$; $^{**}p < 0.01$. In the study, each experimental group (control group and FT group) was composed of 24 P10 CD-1 mice (both sexes) from the same six dams. The granule cell migration of eight mice in each group were observed (1) 12 h after treatment, (2) 24 h after treatment, and (3) 48 h after treatment.

site where cortical layers are undergrown, while FT accelerates granule cell migration in the surroundings of the lesion site where cortical layers are overgrown.

FT alters the translocation of granule cells to the IGL in a lesion site-specific manner

FT-induced alterations of the distance of granule cell migration may affect the translocation of granule cells from their birthplace (the EGL) to their final destination (the IGL), which subsequently alters the growth of the IGL. Using BrdU, which is incorporated only into proliferating cells (e.g., granule cell precursors), we previously reported that in the early postnatal mouse cerebellum, >50% of granule cells translocate their soma from the EGL into the ML, PCL, and IGL within 48 h after their final mitosis at the top of the EGL (Komuro et al., 2001; Kumada et al., 2006). To determine whether FT affects the translocation of granule cells from the EGL to the IGL, we injected BrdU (50 μg/g body weight, i.p.) into control and FT mice 4 h before treatment. Subsequently, using an anti-BrdU monoclonal antibody, we examined the distribution of $BrdU^{+}$ cells in the EGL, ML, and IGL of lobule VIb and crus I of the cerebellum of control and FT mice 48 h after the treatment (Fig. 9*A*). In the FT mice, the average number of $BrdU^{+}$ cells in the ML of the midline region of lobule VIb decreases to 36% of the control mice, while the average number of $BrdU^{+}$ cells in the ML of the proximal region of crus I increases to 116% of the control mice (Fig. 9*B*). Likewise, in the FT mice, the average number of $BrdU^{+}$ cells in the IGL of the midline region of lobule VIb decreases to 31% of the control mice, while the average number of $BrdU^{+}$ cells in the IGL of the proximal region of crus I increases to 113% of the control mice (Fig. 9*C*). These results indicate that FT affects granule cell translocation to the ML and the IGL in a lesion site-specific manner: FT results in the reduction of the number of granule cells reaching the ML and the IGL at the core of the lesion site, but results in the increase of the number of granule cells reaching the ML and the IGL in the surroundings of the lesion site. These results suggest that lesion site-specific alterations of the ML and the IGL growth may be at least in part because of the lesion site-specific alterations of granule cell translocation to the ML and the IGL.

The reduction of the number of granule cells reaching the ML and the IGL at the core of the lesion site may be because of increased cell death of granule cells and granule cell precursors caused by FT. To test this possibility, using a TUNEL assay, we examined apoptotic cell death of granule cell precursors and of granule cells in the EGL and the ML of lobule VIb and crus I of the cerebellum of control and FT mice 48 h after treatment. The TUNEL assay indicated that FT increases cell death in the EGL and the ML of lobule VIb of the cerebellum to 327% of the control mice, but does not significantly affect cell death in the EGL and the ML of crus I (Fig. 10*A*,*B*). These results suggest that the reduction in the number of granule cells reaching the ML and the IGL at the core of the lesion site (lobule VIb) by FT may be because of the inhibition of translocation of granule cells as well

as the increase in cell death of granule cell precursors and granule cells.

Lesion site-specific changes in galanin levels after FT

Our working hypothesis was that FT affects the migration and translocation of granule cells by altering galanin levels. To test this hypothesis, using a galanin ELISA (Sakamoto et al., 2000), we measured galanin levels in lobule VIb and crus I of the cerebellum of control and FT mice 12, 24, and 48 h after treatment. Galanin levels in the midline region of lobule VIb of FT mouse cerebella decreased to 51% (12 h after treatment), 60% (24 h after treatment), and 68% (48 h after treatment) of the control group (Fig. 11*A*). In contrast, galanin levels in the proximal region of crus I of FT mouse cerebella increased to 276% (12 h after treatment), 218% (24 h after treatment), and 132% (48 h after treatment) of the control (Fig. 11*A*). As presented in Figure 11, *B* and *C*, 24 h after FT, Iba1$^+$ cells (microglia/macrophages) and NG2$^+$ cells (oligodendrocyte progenitor cells) in crus I expressed galanin, although these cells do not express galanin in the normal cerebellar cortical layers (Fig. 4*G*,*H*). These results indicated that FT causes the reduction of galanin levels at the core of the lesion site (where granule cell migration decelerates and the number of granule cells reaching the IGL decreases), while FT causes the increase of galanin levels in the surroundings of the lesion site (where granule cell migration accelerates and the number of granule cells reaching the IGL increases), suggesting that lesion site-specific alterations of galanin levels may play a key role in alterations of the migration and translocation of granule cells after injury. The cellular mechanisms underlying the FT-induced alterations of galanin levels remain to be determined.

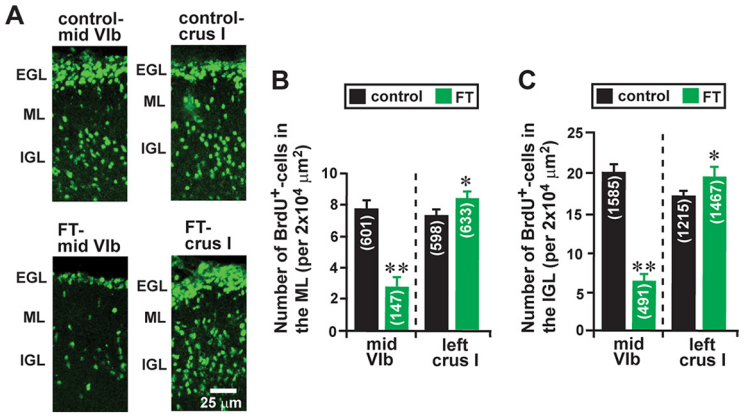

Figure 9. FT-induced alterations of the number of granule cells reaching the ML and the IGL. ***A***, Micrographs showing the distribution of BrdU$^+$ cells in the EGL, the ML, and the IGL of lobule VIb and crus I of the cerebellum of control and FT mice 48 h after treatment. ***B*** and ***C***, Histograms showing the average number of BrdU$^+$ cells in the ML (***B***) and the IGL (***C***) of lobule VIb and crus I of the cerebellum of control and FT mice 48 h after treatment. The number in parentheses in each column indicates the total number of BrdU$^+$ cells counted. Error bars indicate SD. *$p < 0.05$; **$p < 0.01$. The cortical layers (the EGL, the ML, and the IGL) were determined by simultaneously taking transmitted images and fluorescein fluorescent images of each section. In the study, each experimental group (control group and FT group) was composed of five P10 CD-1 mice (both sexes) from the same two dams.

The effects of FT on granule cell migration are reduced by manipulating galanin signaling

If FT affects granule cell migration by altering galanin levels, experimental manipulation of galanin signaling would alter the effects of FT on granule cell migration. To test this possibility, we injected galanin (10 μl of 1 μM) or M40 (5 μl of 1 μM) into the dorsal surface of the cerebellum of the control and FT mice 1, 10, 20, and 40 h after treatment. We measured the migration of granule cells in the EGL of lobule VIb and crus I of the cerebellum of control and FT mice 12, 24, and 48 h after treatment. The injection of galanin into the FT mouse cerebella resulted in an increase of the distance of granule cell migration in the EGL of lobule VIb to 173% (12 h after treatment), 160% (24 h after treatment), and 157% (48 h after treatment) of mice with FT alone, but did not significantly affect the distance of granule cell migration in the EGL of crus I (Fig. 12). On the other hand, the injection of M40 into the FT mouse cerebella resulted in a decrease of the distance of granule cell migration in the EGL of crus I to 76% (12 h after treatment), 79% (24 h after treatment), and 83% (48 h after treatment) of mice with FT alone, but did not significantly affect the distance of granule cell migration in the EGL of lobule VIb (Fig. 12). In both lobule VIb and crus I of control mice, galanin injection increased the distance of granule cell migration in the EGL and M40 injection decreased the distance of granule cell migration in the EGL 12, 24, and 48 h after sham treatment (Fig. 12). These results indicated that stimulating galanin signaling reduces the inhibitory effects of FT on granule cell migration at the core of the lesion site, while inhibiting galanin signaling reduces the stimulatory effects of FT on granule cell migration in the surroundings of the lesion site. These results suggest that lesion site-specific alterations of granule cell migration are at least in part because of the corresponding alterations of galanin levels, implying that FT-induced deficits in neuronal cell migration may be restored by manipulating galanin signaling.

Manipulating galanin signaling mitigates the effects of FT on granule cell translocation and cortical layer growth

The next question was whether manipulating galanin signaling restores FT-induced alterations of granule cell translocation and cortical layer growth. To answer this question, galanin (10 μl of 1 μM) or M40 (5 μl of 1 μM) was injected into the dorsal surface of cerebella of the control and FT mice 1, 10, 20, and 40 h after treatment. To determine the effects of galanin or M40 injection on FT-induced alterations of granule cell translocation and cortical layer growth, 48 h after sham or FT treatment, we examined the distribution of BrdU$^+$ cells in the IGL and the width of cortical layers (in the EGL, ML, and IGL) of lobule VIb and crus I. The injection of galanin increased the number of BrdU$^+$ cells in the IGL of lobule VIb of FT mouse cerebella to 235% of mice with FT alone but did not significantly affect the number of BrdU$^+$ cells in the IGL of crus I (Fig. 13*A*). Likewise, the injection of galanin increased the width of the EGL, ML, and IGL of lobule VIb of FT mouse cerebella to 135%, 123%, and 122% of mice with FT alone, respectively, but did not significantly affect the width of the EGL, ML, and IGL of crus I (Fig. 13*B*). In contrast, the injection of M40 decreased the number of BrdU$^+$ cells in the IGL of crus I of FT mouse cerebella to 75% of mice with FT alone but did not significantly affect the number of BrdU$^+$ cells in the IGL of lobule VIb (Fig. 13*A*). Likewise, the injection of M40 decreased the width of the EGL, ML, and IGL of crus I of FT mouse cerebella to 74%, 87%, and 81% of mice with FT alone, respectively, but did not significantly affect the width of the EGL, ML, and IGL of lobule VIb (Fig. 13*B*). Together, these results

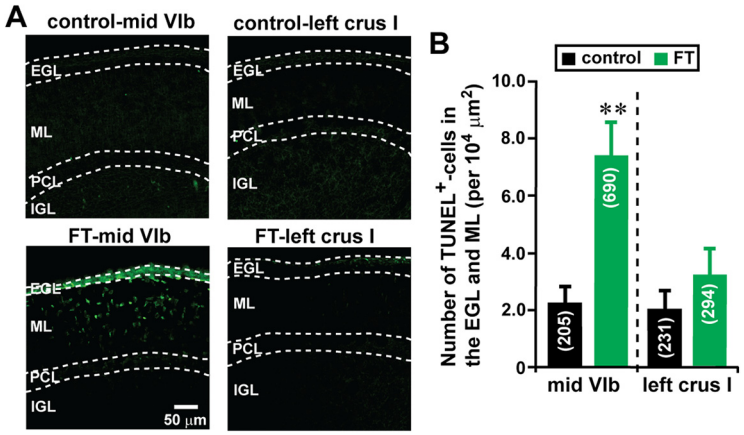

Figure 10. FT increases cell death in the EGL and ML of lobule VIb of the cerebellum, but does not significantly affect cell death in the EGL and ML of crus I. ***A***, Micrographs showing TUNEL$^+$ cells in the EGL and ML of lobule VIb and crus I of the cerebellum of control and FT mice 48 h after treatment. ***B***, Histogram showing the average number of TUNEL$^+$ cells in the EGL and ML of lobule VIb and crus I of the cerebellum of control and FT mice 48 h after treatment. The number in parentheses in each column indicates the total number of TUNEL$^+$ cells counted. Error bars indicate SD. $^{**}p < 0.01$. The cortical layers (the EGL, the ML, and the IGL) were determined by simultaneously taking transmitted images and fluorescein fluorescent images of each section. In the study, each experimental group (control group and FT group) was composed of five P10 CD-1 mice (both sexes) from the same two dams.

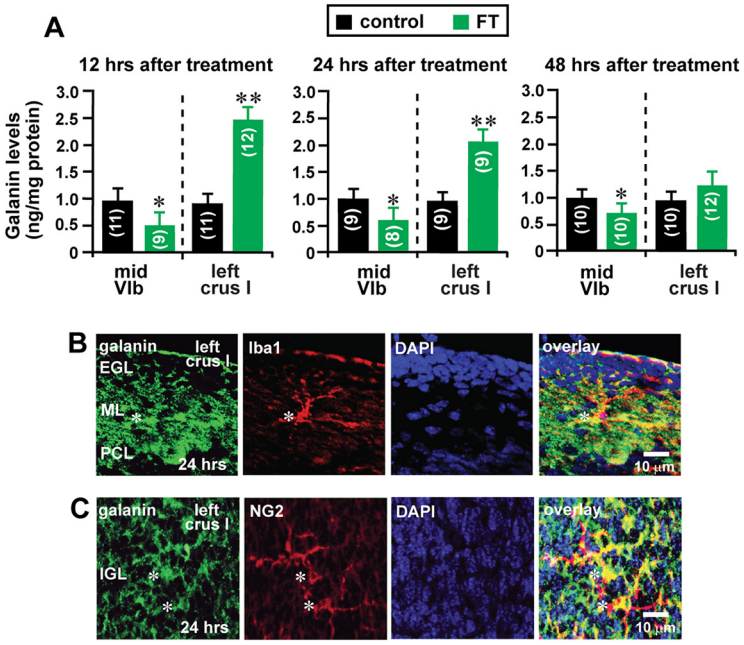

Figure 11. FT alters galanin levels in the early postnatal mouse cerebellum in a lesion site-specific manner. Histograms showing alterations of galanin levels in lobule VIb and crus I in the cerebellum of control and FT mice 12, 24, and 48 h after treatment. The number in parentheses in each column indicates the number of cerebella tested. Error bars represent SD. $^{*}p < 0.05$; $^{**}p < 0.01$. ***A***, In the study, 63 P10 CD-1 mice (both sexes) from seven dams were used. ***B***, Immunostaining of galanin and Iba1 in the EGL, the ML, and the PCL of crus I of the cerebellum of FT mice 24 h after treatment. Asterisks mark the somata of Iba 1$^+$ cells. ***C***, Immunostainings of galanin and NG2 in the IGL of crus I of the cerebellum of FT mice 24 h after treatment. Asterisks mark the somata of NG2$^+$ cells. In this study in ***B*** and ***C***, seven P10 CD-1 mice (both sexes) from two dams were used to conduct immunohistochemical staining.

suggest that lesion site-specific manipulation of galanin signaling may ameliorate FT-induced deficits in granule cell translocation and cortical layer growth.

Discussion

The present study demonstrates that galanin plays a role in controlling the migration of cerebellar granule cells in the early postnatal mouse during normal development and after injury. Galanin maintains the distance of granule cell migration via the activation of its receptors. After cold-induced injury, galanin levels decrease at the core of the lesion site but increase in the surroundings of the lesion site. The lesion site-specific changes in galanin levels result in corresponding changes in the distance of granule cell migration and cortical layer growth. Experimental manipulations of galanin signaling partially ameliorates the effects of cold-induced injury on granule cell migration and cortical layer growth, suggesting that the cold-induced deficits in granule cell migration and cortical layer growth are at least in part because of alterations of galanin levels.

Galanin accelerates granule cell migration via stimulating Ca^{2+} signaling and inhibiting cAMP signaling through the activation of galanin receptors (Fig. 2). In terms of the regulation of Ca^{2+}- and cAMP-signaling activity, GalR1 inhibits forskolin-stimulated cAMP production in a pertussis toxin (PTX)-sensitive manner, opens G-protein-regulated inwardly rectifying K^+ channels, and stimulates mitogen-activated protein kinase (MAPK) activity in a PKC-dependent fashion (Lundström et al., 2005; Lang et al., 2007; Mitsukawa et al., 2008). GalR2 triggers PLC activity and intracellular phosphoinositol turnover, mediating Ca^{2+} release from intracellular Ca^{2+} stores and opening Ca^{2+}-dependent channels (Lundström et al., 2005; Lang et al., 2007). GalR2 also activates MAPK through PKC and may inhibit forskolin-stimulated cAMP production in a PTX-sensitive manner (Lundström et al., 2005; Lang et al., 2007). GalR3 is coupled to the inhibition of AC activity (Lang et al., 2007; Webling et al., 2012; Lang et al., 2015). As described above, all three types of galanin receptors are able to directly or indirectly affect the activity of Ca^{2+} and/or cAMP signaling pathways (Lundström et al., 2005; Lang et al., 2007; Mitsukawa et al., 2008). The precise roles of each galanin receptor in granule cell migration remain to be determined with the combined use of subtype-specific antagonists or agonists of galanin receptors and GalR1-, GalR2-, GalR3-KO (knock-out) mice.

Galanin may play a role in controlling neuronal cell migration in the developing cerebrum. The developing cerebrum expresses high levels of galanin and immature cerebral cortical neurons express galanin receptors (Fig. 5*G*; Elmquist et al., 1993; Burazin et al., 2000; Shen et al., 2005). The migration of cerebral cortical neurons is also controlled

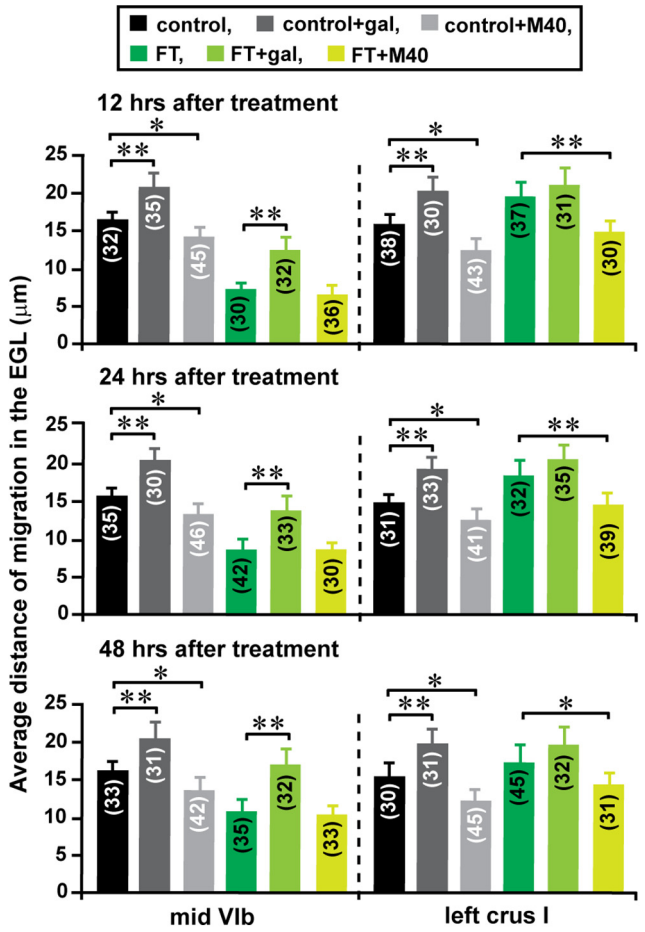

Figure 12. Manipulation of galanin signaling by injecting galanin and M40 ameliorates the effects of FT on granule cell migration. Histograms showing the effects of the injection of galanin or M40 into the dorsal surface of the cerebella on the average distance of granule cell migration during the 1 h period in the EGL in lobule VIb and crus I in the cerebellum of control and FT mice 12, 24, and 48 h after treatment. The number in parentheses in each column indicates the number of granule cells tested. Error bars indicate SD. *$p < 0.05$; **$p < 0.01$. In the study, each experimental group (1, control group; 2, control + galanin group; 3, control + M40 group; 4, FT group; 5, FT + galanin group; 6, FT + M40 group) was composed of 15 P10 CD-1 mice (both sexes) from the same 12 dams. Five mice in each experimental group were tested for granule cell migration (1) 12 h after treatment, (2) 24 h after treatment, and (3) 48 h after treatment, respectively.

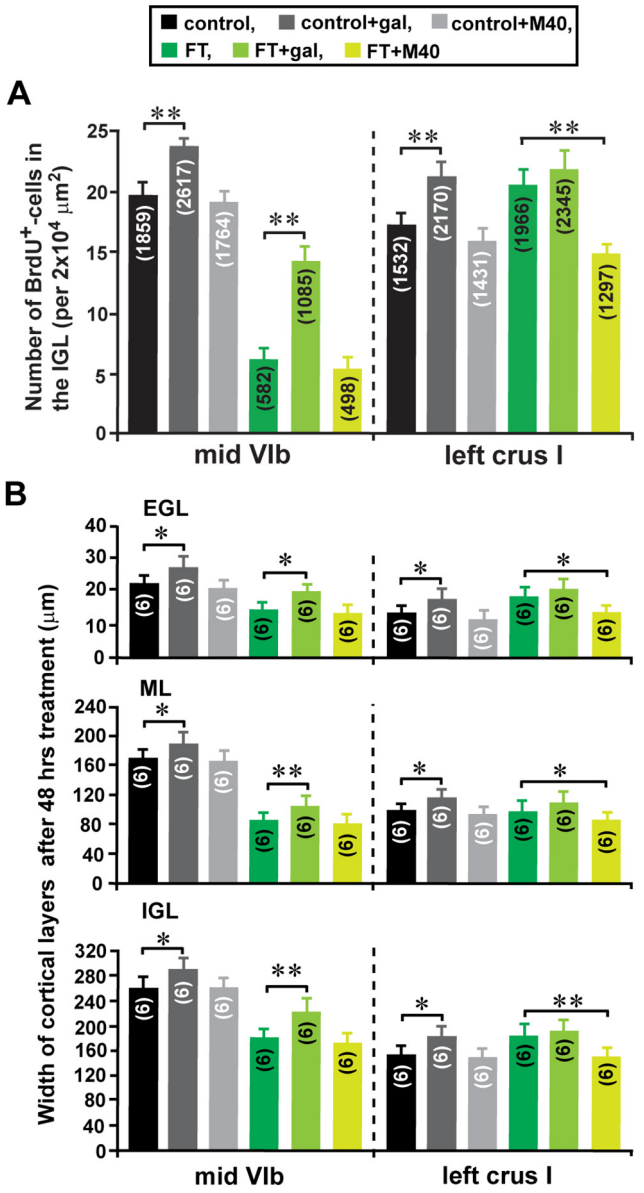

Figure 13. ***A***, ***B***, Manipulation of galanin signaling by injecting galanin and M40 reduces the effects of FT on the translocation of granule cells (***A***) and the growth of cerebellar cortical layers (***B***). ***A***, Histograms showing the effects of the injection of galanin and M40 into the dorsal surface of the cerebella on the average number of $BrdU^+$ cells in the IGL of lobule VIb and crus I of the cerebellum of control and FT mice 48 h after treatment. The number in parentheses in each column indicates the total number of $BrdU^+$ cells counted. ***B***, Histograms showing the effects of the injection of galanin and M40 into the dorsal surface of the cerebella on the average width of the EGL, ML, and IGL of lobule VIb and crus I of the cerebellum of control and FT mice 48 h after treatment. The number in parentheses in each column indicates the number of mice tested. In ***A*** and ***B***, error bars indicate SD. *$p < 0.05$; **$p < 0.01$. In the study, each experimental group (1, control group; 2, control + galanin group; 3, control + M40 group; 4, FT group; 5, FT + galanin group; 6, FT + M40 group) was composed of six P10 CD-1 mice (both sexes) from the same six dams.

by alterations of the Ca^{2+} and cAMP signaling pathways (Behar et al., 1996; Lundgren et al., 2012; Bony et al., 2013). Collectively, these lines of evidence suggest that galanin may control the migration of cerebral cortical neurons during normal development.

There are some discrepancies in the effects of M40 (a nonspecific galanin receptor antagonist) on granule cell migration in this study. The application of M40 did not alter the distance of granule cell migration in the microexplant cultures (Fig. 2*A*), while the application of M40 reduced the distance of granule cell migration in the cerebellar slice preparations (Fig. 3*E*). There is a possible scenario that explains the discrepancies. In the microexplant cultures of early postnatal mouse cerebella, >95% of the cells are cerebellar granule cells (Yacubova and Komuro, 2002), and galanin-producing cells (e.g., Purkinje cells and Golgi cells) are very rare (Nagata and Nakatsuji, 1990). The culture medium used for microexplant cultures (Neurobasal Medium with N2 supplement) does not contain galanin. The lines of evidence suggest that in the microexplant cultures, galanin receptors on migrating granule cells may not be activated because of low levels of galanin in the surrounding microenvironment, leading to the lack of the effects of M40 on migration. In contrast, in the cerebellar slice preparations, which contain galanin-producing cells and processes (including Purkinje cells, Golgi cells, and mossy rosettes), galanin receptors on migrating granule cells may be activated because of high levels of galanin in the surrounding microenvironment, leading to the inhibitory effects of M40 on migration.

During the migration from the EGL through the ML and the PCL to the IGL, granule cells exhibit three different modes of migration (1, tangential migration in the EGL; 2, glia-associated radial migration in the ML; 3, glia-independent radial migration in the IGL; Komuro and Rakic, 1995, 1998a; Komuro et al., 2001). It has been suggested that the modes of neuronal migration are determined by the expression of cell-adhesion molecules and guidance molecules (including attractive and repulsive molecules), and physical contacts between migrating cells and surrounding tissues (Komuro and Rakic, 1998b; Yacubova and Komuro, 2003; Togashi et al., 2009; Solecki, 2012; Minegishi and Inagaki, 2020). In this study, the application of galanin or M40 alters the distance of granule cell migration, but the galanin- and M40-induced changes in migration do not depend on the mode of migration (Fig. 3*E*), suggesting that galanin and its receptor are primarily involved in controlling the motility of granule cells.

Global galanin KO mice exhibit a wide variety of phenotypes, including endocrine, neurologic, and behavioral deficits (Wynick et al., 1998; Holmes et al., 2000; Wynick and Bacon, 2002; Zachariou et al., 2003; Ahrén et al., 2004; Adams et al., 2008). Galanin-KO mice, GalR1-KO mice, and GalR2-KO mice do not display any marked phenotype in the neuronal cytoarchitecture in the CNS (Lang et al., 2015). These findings suggest that the effects of the loss of galanin signaling on brain development may be compensated for by the upregulation of other signaling and that galanin signaling may not be essential for the maintenance of neuronal cell migration and cortical layer growth during normal brain development. Conversely, galanin-KO mice demonstrate a 35% reduction of the number of DRG neurons after nerve injury compared with WT controls (Holmes et al., 2000), suggesting that galanin signaling may play a critical role in the recovery and survival of neurons after injury.

Brain injury during prenatal and early postnatal development remains a significant health problem, and often leads to functional and morphologic deficits in developing brains (Soto-Ares et al., 2000; Rutherford et al., 2010, 2012; Back and Miller, 2014). Therapeutic interventions aimed at facilitating morphologic and functional recovery are limited. It has been shown that galanin gene expression and peptide secretion in the nervous system are upregulated by traumatic brain injury, ischemia, seizure, and axotomy (Cortés et al., 1990; Hökfelt et al., 1994; Burazin and Gundlach, 1998; Liu and Hökfelt, 2000; Lundström et al., 2005; Lang et al., 2007; Mitsukawa et al., 2008; Holm et al., 2011, 2012; Webling et al., 2012). In this study, to examine whether galanin signaling is involved in the deficits in neuronal cell migration and cortical layer growth after brain injury, we chose FT (Peiffer et al., 2003; Scantlebury et al., 2004; Chiaretti et al., 2011; Wang et al., 2014). It has been shown that FT induces microgyrus in the developing cerebrum, a focal cortical malformation with a small sulcus, and a three- or four-layered microgyric cortex, which resembles human four-layered microgyria (Dvorák and Feit, 1977; Dvorõàk et al., 1978). Interestingly, the microgyric cortex is formed only during the period of active neuronal cell migration (Dvorák and Feit, 1977), suggesting that FT provides the best model system to examine the role of galanin in the neuronal cell migration and cortical layer growth after injury.

FT induces the alterations of galanin levels in a lesion site-specific manner (Fig. 11*A*). The downregulation of galanin levels at the core of the lesion site may be because of damage to or cell death of galanin-expressing cells (e.g., Purkinje cells), leading to the reduction of galanin synthesis. The upregulation of galanin levels in the surroundings of the lesion site remain to be determined, but there are some hints. It has been reported that, after injury, $NG2^+$ cells and microglia often start to express galanin (Hwang et al., 2004; Butzkueven and Gundlach, 2010). The present results also show the expression of galanin in $NG2^+$ cells and $Iba1^+$ cells in lobule crus I (Fig. 11*B*). Furthermore, it has been suggested that the leukemia inhibitory factor secreted by astrocytes plays a key role in the upregulation of galanin in glia and neurons after injury (Holmberg and Patterson, 2006). Collectively, these lines of evidence suggest that the upregulation of galanin levels in the surroundings of the lesion site may be because of (1) an increase in the number of galanin-expressing cells, (2) enhanced galanin synthesis in neurons and glia, and (3) the combination of 1 and 2.

The alterations of galanin levels after injury may play multiple roles in cortical layer growth. It has been reported that galanin stimulates neuronal cell proliferation and inhibits apoptotic cell death (Mazarati et al., 2004; Abbosh et al., 2011), implying that FT-induced alterations of cortical layer growth may result from the sum of complicated effects of galanin on proliferation, migration, and cell death.

The question of whether the manipulation of galanin signaling ameliorates the adverse effects of widespread brain injury on neuronal cell migration and cortical layer growth remains to be determined. The present study sheds light on the role of galanin in searching for potential therapeutic treatments for infants with focal brain injury.

References

Abbosh C, Lawkowski A, Zaben M, Gray W (2011) GalR2/3 mediates proliferative and trophic effects of galanin on postnatal hippocampal precursors. J Neurochem 117:425–436.

Adams AC, Clapham JC, Wynick D, Speakman JR (2008) Feeding behaviour in galanin knockout mice supports a role of galanin in fat intake and preference. J Neuroendocrinol 20:199–206.

Ahrén B, Pacini G, Wynick D, Wierup N, Sundler F (2004) Loss-of-function mutation of the galanin gene is associated with perturbed islet function in mice. Endocrinology 145:3190–3196.

Back SA, Miller SP (2014) Brain injury in premature neonates: a primary cerebral dysmaturation disorder? Ann Neurol 75:469–486.

Behar TN, Li YX, Tran HT, Ma W, Dunlap V, Scott C, Barker JL (1996) GABA stimulates chemotaxis and chemokinesis of embryonic cortical neurons via calcium-dependent mechanisms. J Neurosci 16:1808–1818.

Bony G, Szczurkowska J, Tamagno I, Shelly M, Contestabile A, Cancedda L (2013) Non-hyperpolarizing $GABA_B$ receptor activation regulates neuronal migration and neurite growth and specification by cAMP/LKB1. Nat Commun 4:1800.

Burazin TC, Gundlach AL (1998) Inducible galanin and GalR2 receptor system in motor neuron injury and regeneration. J Neurochem 71:879–882.

Burazin TC, Larm JA, Ryan MC, Gundlach AL (2000) Galanin-R1 and -R2 receptor mRNA expression during the development of rat brain suggests differential subtype involvement in synaptic transmission and plasticity. Eur J Neurosci 12:2901–2917.

Butzkueven H, Gundlach AL (2010) Galanin in glia: expression and potential role in the CNS. Exp Suppl 102:61–69.

Cameron DB, Galas L, Jiang L, Raoult E, Vaudry D, Komuro H (2007) Cerebellar cortical layer-specific control of neuronal migration by PACAP. Neuroscience 146:697–712.

Chiaretti A, Narducci A, Novegno F, Antonelli A, Pierri F, Fantacci C, Di Rocco C, Tamburrini G (2011) Effects of nerve growth factor in experimental model of focal microgyria. Childs Nerv Syst 27:2117–2122.

Cortés R, Villar MJ, Verhofstad A, Hökfelt T (1990) Effects of central nervous system lesions on the expression of galanin: a comparative in situ hybridization and immunohistochemical study. Proc Natl Acad Sci U S A 87:7742–7746.

Dvorák K, Feit J (1977) Migration of neuroblasts through partial necrosis of the cerebral cortex in newborn rats-contribution to the problems of morphological development and developmental period of cerebral

microgyria. Histological and autoradiographical study. Acta Neuropathol 38:203–212.
Dvorõàk K, Feit J, Juránková Z (1978) Experimentally induced focal microgyria and status verrucosus deformis in rats–pathogenesis and interrelation. Histological and autoradiographical study. Acta Neuropathol 44:121–129.
Elmquist JK, Kao A, Kuehl-Kovarik MC, Jacobson CD (1993) Developmental profile of galanin binding sites in the mammalian brain. Mol Cell Neurosci 4:354–365.
Fahrion JK, Komuro Y, Li Y, Ohno N, Littner Y, Raoult E, Galas L, Vaudry D, Komuro H (2012) Rescue of neuronal migration deficits in a mouse model of fetal minamata disease by increasing neuronal Ca^{2+} spike frequency. Proc Natl Acad Sci U S A 109:5057–5062.
Flint AC, Kriegstein AR (1997) Mechanisms underlying neuronal migration disorders and epilepsy. Curr Opin Neurol 10:92–97.
Guipponi M, Chentouf A, Webling KEB, Freimann K, Crespel A, Nobile C, Lemke JR, Hansen J, Dorn T, Lesca G, Ryvlin P, Hirsch E, Rudolf G, Rosenberg DS, Weber Y, Becker F, Helbig I, Muhle H, Salzmann A, Chaouch M, et al. (2015) Galanin pathogenic mutations in temporal lobe epilepsy. Hum Mol Genet 24:3082–3091.
Hewitt SM, Baskin DG, Frevert CW, Stahl WL, Rosa-Molinar E (2014) Controls for immunohistochemistry: the Histochemical Society's standards of practice for validation of immunohistochemical assays. J Histochem Cytochem 62:693–697.
Hökfelt T, Zhang X, Wiesenfeld-Hallin Z (1994) Messenger plasticity in primary sensory neurons following axotomy and its functional implications. Trends Neurosci 17:22–30.
Holm L, Theodorsson E, Hökfelt T, Theodorsson A (2011) Effects of intracerebroventricular galanin or a galanin receptor 2/3 agonist on the lesion induced by transient occlusion of the middle cerebral artery in female rats. Neuropeptides 45:17–23.
Holm L, Hilke S, Adori C, Theodorsson E, Hökfelt T, Theodorsson A (2012) Changes in galanin and GalR1 gene expression in discrete brain regions after transient occlusion of the middle cerebral artery in female rats. Neuropeptides 46:19–27.
Holmberg KH, Patterson PH (2006) Leukemia inhibitory factor is a key regulator of astrocytic, microglial and neuronal responses in a low-dose pilocarpine injury model. Brain Res 1075:26–35.
Holmes FE, Mahoney S, King VR, Bacon A, Kerr NCH, Pachnis V, Curtis R, Priestley JV, Wynick D (2000) Targeted disruption of the galanin gene reduces the number of sensory neurons and their regenerative capacity. Proc Natl Acad Sci U S A 97:11563–11568.
Hwang IK, Yoo KY, Kim DS, Do SG, Oh YS, Kang TC, Han BH, Kim JS, Won MH (2004) Expression and changes of galanin in neurons and microglia in the hippocampus after transient forebrain ischemia in gerbils. Brain Res 1023:193–199.
Jiang L, Kumada T, Cameron DB, Komuro H (2008) Cerebellar granule cell migration and the effects of alcohol. Dev Neurosci 30:7–23.
Jungnickel SR, Yao M, Shen PJ, Gundlach AL (2005) Induction of galanin receptor-1 (GalR1) expression in external granule cell layer of post-natal mouse cerebellum. J Neurochem 92:1452–1462.
Kinney JW, Starosta G, Holmes A, Wrenn CC, Yang RJ, Harris AP, Long KC, Crawley JN (2002) Deficits in trace cued fear conditioning in galanin-treated rats and galanin-overexpressing transgenic mice. Learn Mem 9:178–190.
Komuro H, Kumada T (2005) Ca^{2+} transients control CNS neuronal migration. Cell Calcium 37:387–393.
Komuro H, Rakic P (1993) Modulation of neuronal migration by NMDA receptors. Science 260:95–97.
Komuro H, Rakic P (1995) Dynamics of granule cell migration: a confocal microscopic study in acute cerebellar slice preparations. J Neurosci 15:1110–1120.
Komuro H, Rakic P (1996) Intracellular Ca^{2+} fluctuations modulate the rate of neuronal migration. Neuron 17:275–285.
Komuro H, Rakic P (1998a) Distinct modes of neuronal migration in different domains of developing cerebellar cortex. J Neurosci 18:1478–1490.
Komuro H, Rakic P (1998b) Orchestration of neuronal migration by activity of ion channels, neurotransmitter receptors and intracellular Ca^{2+} fluctuations. J Neurobiol 37:110–130.
Komuro H, Yacubova E (2003) Recent advances in cerebellar granule cell migration. Cell Mol Life Sci 60:1084–1098.
Komuro H, Yacubova E, Yacubova E, Rakic P (2001) Mode and tempo of tangential cell migration in the cerebellar external granular layer. J Neurosci 21:527–540.
Komuro Y, Kumada T, Ohno N, Foote KD, Komuro H (2013) Migration in the cerebellum. In: Cellular migration and formation of neuronal connection (Rubenstein J, Rakic P, eds), pp 281–298. New York: Elsevier.
Komuro Y, Galas L, Lebon A, Raoult E, Fahrion JK, Tilot A, Kumada T, Ohno N, Vaudry D, Komuro H (2015) The role of calcium and cyclic nucleotide signaling in cerebellar granule cell migration. Dev Neurobiol 75:369–387.
Kumada T, Komuro H (2004) Completion of neuronal migration regulated by loss of Ca^{2+} transients. Proc Natl Acad Sci U S A 101:8479–8484.
Kumada T, Lakshmana ML, Komuro H (2006) Reversal of neuronal migration in a mouse model of fetal alcohol syndrome by controlling second messenger signaling. J Neurosci 26:742–756.
Kumada T, Jiang Y, Kawanami A, Cameron DB, Komuro H (2009) Autonomous turning of cerebellar granule cells in vitro by intrinsic programs. Dev Biol 326:237–249.
Lang R, Gundlach AL, Kofler B (2007) The galanin peptide family: receptor pharmacology, pleiotropic biological actions, and implications in health and disease. Pharmacol Ther 115:177–207.
Lang R, Gundlach AL, Holmes FE, Hobson SA, Wynick D, Hökfelt T, Kofler B (2015) Physiology, signaling, and pharmacology of galanin peptides and receptors: three decades of emerging diversity. Pharmacol Rev 67:118–175.
Li Y, Komuro Y, Fahrion JK, Hu T, Ohno N, Fenner KB, Wooton J, Raoult E, Galas L, Vaudry D, Komuro H (2012) Light stimuli control neuronal migration by altering of insulin-like growth factor 1 (IGF-1) signaling. Proc Natl Acad Sci U S A 109:2630–2635.
Liu T, Hökfelt T (2000) Effect of intrathecal galanin and its putative antagonist M35 on pain behavior in a neuropathic pain model. Brain Res 886:67–72.
Lundgren TK, Nakahata K, Fritz N, Rebellato P, Zhang S, Uhlén P (2012) RET PLCγ phosphotyrosine binding domain regulates Ca^{2+} signaling and neocortical neuronal migration. PLoS One 7:e31258.
Lundström L, Elmquist A, Bartfai T, Langel U (2005) Galanin and its receptors in neurological disorders. Neuromolecular Med 7:157–180.
Manent JB, Wang Y, Chang Y, Paramasivam M, LoTurco JJ (2009) Dcx reexpression reduces subcortical band heterotopia and seizure threshold in an animal model of neuronal migration disorder. Nat Med 15:84–90.
Mahoney SA, Hosking R, Farrant S, Holmes FE, Jacoby AS, Shine J, Iismaa TP, Scott MK, Schmidt R, Wynic D (2003) The second galanin receptor GalR2 plays a key role in neurite outgrowth from adult sensory neurons. J Neurosci 23:416–421.
Marín O, Rubenstein JL (2003) Cell migration in the forebrain. Annu Rev Neurosci 26:441–483.
Mazarati A, Lu X, Kilk K, Langel U, Wasterlain C, Bartfai T (2004) Galanin type 2 receptors regulate neuronal survival, susceptibility to seizures and seizure-induced neurogenesis in the dentate gyrus. Eur J Neurosci 19:3235–3244.
Mazarati AM (2004) Galanin and galanin receptors in epilepsy. Neuropeptides 38:331–343.
Miale I, Sidman RL (1961) An autoradiographic analysis of histogenesis in the mouse cerebellum. Exp Neurol 4:277–296.
Minegishi T, Inagaki N (2020) Forces to drive neuronal migration steps. Front Cell Dev Biol 8:863.
Mitsukawa K, Lu X, Bartfai T (2008) Galanin, galanin receptors and drug targets. Cell Mol Life Sci 65:1796–1805.
Nagata I, Nakatsuji N (1990) Granule cell behavior on laminin in cerebellar microexplant cultures. Brain Res Dev Brain Res 52:63–73.
Peiffer AM, Fitch RH, Thomas JJ, Alexandra N, Yurkovic AN, Glenn D Rosen GD (2003) Brain weight differences associated with induced focal microgyria. BMC Neurosci 4:12.
Rakic P (1971) Neuron-glia relationship during granule cell migration in developing cerebellar cortex. A Golgi and electronmicroscopic study in Macacus Rhesus. J Comp Neurol 141:283–312.
Rakic P (1990) Principles of neural cell migration. Experientia 46:882–891.
Rakic P, Komuro H (1995) The role of receptor/channel activity in neuronal cell migration. J Neurobiol 26:299–315.
Rakic P, Cameron SR, Komuro H (1994) Recognition, adhesion, transmembrane signaling and cell motility in guided neuronal migration. Curr Opin Neurobiol 4:63–69.

Raoult E, Bénard M, Komuro H, Lebon A, Vivien D, Fournier A, Vaudry H, Vaudry D, Galas L (2014) Cortical-layer-specific effects of PACAP and tPA on interneuron migration during post-natal development of the cerebellum. J Neurochem 130:241–254.

Raoult E, Roussel B, Bénard M, Lefebvre T, Ravni A, Ali C, Vivien D, Komuro H, Fournier A, Vaudry H, Vaudry D, Galas L (2011) Pituitary adenylate cyclase-activating polypeptide (PACAP) stimulates the expression and the release of tissue plasminogen activator (tPA) in neuronal cells. Involvement of tPA in neuroprotective effect of PACAP. J Neurochem 119:920–931.

Rutherford MA, Biarge MM, Allsop J, Counsell S, Cowan FM (2010) MRI of perinatal brain injury. Pediatr Radiol 40:819–833.

Rutherford MA, Ramenghi LA, Cowan FM (2012) Neonatal stroke. Arch Dis Child Fetal Neonatal Ed 97:F377–384.

Ryan MC, Loiacono RE, Gundlach AL (1997) Galanin messenger RNA during postnatal development of the rat brain: expression patterns in Purkinje cells differentiate anterior and posterior lobes of cerebellum. Neuroscience 78:1113–1127.

Sakamoto H, Ubuka T, Kohchi C, Li D, Ukena K, Tsutsui K (2000) Existence of galanin in lumbosacral sympathetic ganglionic neurons that project to the quail uterine oviduct. Endocrinology 141:4402–4412.

Scantlebury MH, Ouellet P-L, Psarropoulou C, Lionel Carmant L (2004) Freeze lesion–induced focal cortical dysplasia predisposes to atypical hyperthermic seizures in the immature rat. Epilepsia 45:592–600.

Shen PJ, Gundlach AL (2010) Galanin systems and ischemia: peptide and receptor plasticity in neurons and oligodendroglial precursors. Exp Suppl 102:209–221.

Shen PJ, Larm JA, Gundlach AL (2003) Expression and plasticity of galanin systems in cortical neurons, oligodendrocyte progenitors and proliferative zones in normal brain and after spreading depression. Eur J Neurosci 18:1362–1376.

Shen P-J, Yuan C-G, Ma J, Cheng S, Yao M, Turnley AM, Gundlach AL (2005) Galanin in neuro(glio)genesis: expression of galanin and receptors by progenitor cells in vivo and in vitro and effects of galanin on neurosphere proliferation. Neuropeptides 39:201–205.

Solecki D (2012) Sticky situations: recent advances in control of cell adhesion during neuronal migration. Curr Opin Neurobiol 22:791–798.

Soto-Ares G, Delaire C, Deries B, Vallee L, Pruvo JP (2000) Cerebellar cortical dysplasia: MR findings in a complex entity. Am J Neuroradiol 21:1511–1519.

Steiner RA, Hohmann JG, Holmes A, Wrenn CC, Cadd G, Juréus A, Clifton DK, Luo M, Gutshall M, Ma SY, Mufson EJ, Crawley J (2001) Galanin transgenic mice display cognitive and neurochemical deficits characteristic of Alzheimer's disease. Proc Natl Acad Sci U S A 98:4184–4189.

Togashi H, Sakisaka T, Takai Y (2009) Cell adhesion molecules in the central nervous system. Cell Adh Migr 3:29–35.

Valiente M, Marín O (2010) Neuronal migration mechanisms in development and disease. Curr Opin Neurobiol 20:68–78.

Wang T, Kumada T, Morishima T, Iwata S, Kaneko T, Yanagawa Y, Yoshida S, Fukuda A (2014) Accumulation of GABAergic neurons, causing a focal ambient GABA gradient, and downregulation of KCC2 are induced microgyrus formation in a mouse model of polymicrogyria. Cereb Cortex 24:1088–1101.

Webling KEB, Runesson J, Bartfai T, Langel U (2012) Galanin receptors and ligands. Front Endocrinol (Lausanne) 3:146.

Wynick D, Bacon A (2002) Targeted disruption of galanin: new insights from knock-out studies. Neuropeptides 36:132–144.

Wynick D, Small CJ, Bacon A, Holmes FE, Norman M, Ormandy CJ, Kilic E, Kerr NCH, Ghatei M, Talamantes F, Bloom SR, Pachnis V (1998) Galanin regulates prolactin release and lactotroph proliferation. Proc Natl Acad Sci U S A 95:12671–12676.

Yacubova E, Komuro H (2002) Intrinsic program for migration of cerebellar granule cells *in vitro*. J Neurosci 22:5966–5981.

Yacubova E, Komuro H (2003) Cellular and molecular mechanisms of cerebellar granule cell migration. Cell Biochem Biophys 37:213–234.

Zachariou V, Brunzell DH, Hawes J, Stedman DR, Bartfai T, Steiner RA, Wynick D, Langel U, Picciotto MR (2003) The neuropeptide galanin modulates behavioral and neurochemical signs of opiate withdrawal. Proc Natl Acad Sci U S A 100:9028–9033.